LBL-29696
UC-210

Lawrence Berkeley Laboratory
UNIVERSITY OF CALIFORNIA

APPLIED SCIENCE DIVISION

Electrocatalysts for Oxygen Electrodes: Final Report

E. Yeager

October 1990

APPLIED SCIENCE DIVISION

LOAN COPY
Circulates
for 2 weeks
Bldg. 50 Library.
LBL-29696
Copy 2

Prepared for the U.S. Department of Energy under Contract Number DE-AC03-76SF00098.

DISCLAIMER

This document was prepared as an account of work sponsored by the United States Government. While this document is believed to contain correct information, neither the United States Government nor any agency thereof, nor the Regents of the University of California, nor any of their employees, makes any warranty, express or implied, or assumes any legal responsibility for the accuracy, completeness, or usefulness of any information, apparatus, product, or process disclosed, or represents that its use would not infringe privately owned rights. Reference herein to any specific commercial product, process, or service by its trade name, trademark, manufacturer, or otherwise, does not necessarily constitute or imply its endorsement, recommendation, or favoring by the United States Government or any agency thereof, or the Regents of the University of California. The views and opinions of authors expressed herein do not necessarily state or reflect those of the United States Government or any agency thereof or the Regents of the University of California.

LBL-29696

ELECTROCATALYSTS FOR OXYGEN ELECTRODES

Final Report

October 1990

by

Ernest Yeager

Case Center for Electrochemical Sciences
and the Department of Chemistry
Case Western Reserve University
Cleveland, Ohio 44106-2099

for

Technology Base Research Project
Applied Science Division
Lawrence Berkeley Laboratory
Berkeley, California 94720

This work was supported by the Assistant Secretary for Conservation and Renewable Energy, Deputy Assistant Secretary for Utility Technologies, Office of Energy Management, Advanced Utility Concepts Division of the U.S. Department of Energy under Contract No. DE-AC03-76SF00098, Subcontract No. 4544410 with the Lawrence Berkeley Laboratory.

PREFACE

This annual report is a comprehensive summary of the results obtained during the past year. The following personnel were involved in the research on a full or part time basis.

W. Aldred	Research Assistant
I. Bae	Graduate Student
R. Chen	Graduate Student
H. Huang	Graduate Student
S. Gupta*	Senior Research Associate
J. Prakash	Graduate Student
D. Tryk	Senior Research Associate
Z. Zheng	Visiting Scientist
E. Yeager	Project Director

*Report prepared by S. Gupta.

TABLE OF CONTENTS

PREFACE v

TABLE OF CONTENTS vii

I. SUMMARY 1

II. OBJECTIVES 7

III. INTRODUCTION 7

IV. ACCOMPLISHMENTS 8

A. Electrochemical and spectroscopic studies of transition metal macrocycle catalysts 8

A-1. Adsorption of the tetrasulfonated phthalocyanines on ordinary pyrolytic graphite substrate 9

A-2. Adsorption of tetrasulfonated phthalocyanines on highly ordered pyrolytic graphite (HOPG) 18

A-3. Adsorption of tetrasulfonated phthalocyanines on Pt and Au surfaces 20

A-4. Cyclic voltammetry and O_2 electrocatalytic studies of TsPc's adsorbed on polycrystalline Ag in acid and alkaline solutions 22

B. STM and high-resolution TEM studies of monomeric and sheet-polymeric phthalocyanines 23

B-1. STM studies 25

B-2. TEM studies 26

C. Adsorbed layers of dimeric macrocycles designed to test the "dry cave" concept 27

D. Controlled poisoning of transition metal macrocycles by CO 29

E. Polymer-modified electrodes 29

F. Transition metal oxide catalysts: pyrochlores and lithiated NiO 48

F-1. Pyrochlores 48

F-2. Lithiated NiO 49

G. Electrocatalysts for bifunctional electrodes 50

G-1. Pyrochlores (use of pore-former) 50

G-2. Preparation of pyrochlore with other platinum group metals substituted for ruthenium 51

G-3. Iron-ruthenium perovskites as catalysts for bifunctional electrodes 51

H. Catalyst supports 53

V. FUTURE WORK 56

VI. REFERENCES 57

I. SUMMARY

The overall objective of this research was an in-depth understanding of the factors controlling O_2 reduction and generation on various electrocatalysts and the use of this understanding to identify much higher activity, stable catalysts. The following is a brief summary of the research for the period 1 April 1989 to 31 March 1990.

1. Transition metal monomeric and sheet-polymeric macrocycle catalysts

The iron tetrasulfonated phthalocyanine (FeTsPc) complex adsorbed on an electrode surface has high activity for the 4-electron reduction of O_2 to water or OH^- in alkaline solutions. The configuration of the complex on the surface has a strong effect on the activity as well as pathway but is not well understood. The subcontract research has focused on this problem using electrochemical and in-situ spectroscopic tehcniques [UV-visible, FTIR, Raman (SERS, RR)and Mossbauer]. The measurements indicate that the configuration of the adsorbed complex depends on the electrolyte from which it is adsorbed, particularly the pH. UV-visible absorption spectroscopic studies present evidence that the FeTsPc is present in the μ-oxo form in pure water or alkaline solutions. When the FeTsPc is adsorbed on ordinary pyrolytic graphite (OPG) surfaces from acid solutions, there is no evidence of a μ-oxo form. The adsorption studies of these compounds were extended to other well-defined surfaces including highly ordered pyrolytic graphite (HOPG), platinum and gold. The nature of the substrate, the acidity, the presence of O_2 and the particular transition metal cation, all play an important role in controlling the structure of the adsorbed layer. For a platinum electrode in acid electrolyte, the hyrogen adsorption and the double layer capacitance were decreased in the presence of the TsPc's in solution while cycling in the potential range -0.27 to + 0.40 V vs. SCE. This supports the adsorption of FeTsPc on Pt. This feature disappeared upon potential change to the Pt anodic film region. The

difference in the calculated charge for hydrogen adsorption in the absence and in the presence of FeTsPc on the surface indicated that ~40% of the Pt surface was still available for hydrogen adsorption at the saturation coverage of FeTsPc, in agreement with the STM image obtained by Lippel and coworkers which showed a significant intermolecular void space at monolayer coverge.

A gold electrode prepared by vapor deposition was tested in the Au double-layer region (-0.40 V to +1.0 V in 0.1 M $HClO_4$) for adsorption of these compounds in the same fashion but no evidence for adsorption was found.

The adsorption of these compounds was also studied on mechanically polished polycrystalline silver electrode in acid and alkaline solutions as the silver electrode has a special interest because of its use in the Raman studies (SERS effects) of adsorbed transition metal macrocycles. Well-defined voltammetric peaks in acid electrolyte were obtained whereas no peaks were observed in alkaline solution. The FeTsPc generally gives four well-defined voltammetric peaks on OPG depending on pH of the electrolyte. However, only two peaks at cathodic potentials were obtained with an Ag electrode in acid solution because the Ag is oxidized at relatively low positive potentials. FeTsPc and CoTsPc adsorbed on Ag increased the catalytic activity for O_2 reduction in alkaline solution (shift the polarization by ~100 mV positive) even though Ag is itself a moderately active catalyst for this reaction. No catalytic effect for O_2 reduction was found for FeTsPc and CoTsPc adsorbed on Ag electrodes in 0.05 M H_2SO_4.

Studies on the adsorbed layers of dimeric macrocycles, designed to test the "dry cave" concept were initiated during the past year. The important feature of this work is that the cavity formed by the mixture of the oppositely charged water or ethanol soluble macrocycles may be hydrophobic enough to favor the adsorption of O_2 and enhance the kinetics for O_2 reduction.

Positively charged tetra kis(4-trimethyl ammonium phenyl) porphyrin (TTAPP) and negatively charged tetra kis (sulfonated phenyl) porphyrin (TSPP) with cobalt ion were synthesized and characterized by UV-visible and diffuse reflectance FTIR spectroscopy. Mixtures of the aqueous solutions of the two oppositely charged porphyrins gave a precipitate which was also characterized by the same spectroscopic techniques. These studies indicated an interaction between the macrocycles through sulfonic and ammonium-phenyl groups. Cyclic voltammetry and O_2 reduction electrocatalytic activity for these monomers and their dimer adsorbed on HOPG surface are under investigation.

Research was initiated in the use of the scanning tunneling microscope (Nanoscope II) for ex-situ and in-situ layers of adsorbed monomeric and sheet-polymeric phthalocyanines including the TsPc's on various low index single crystal surfaces (HOPG, Pt and Au) at B.P. America. A crystalline structure was observed for polymeric CuPc adsorbed on HOPG in multilayer coverage. Recently a Digital Instruments Nanoscope II has been obtained in our laboratory and set up for the use of in-situ electrochemical measurements. We should have sufficient resolution but preventing perturbation of the adsorbate and the surface by the scanning tip may be a problem. These effects may be less of a problem with in-situ measurements.

Transmission electron microscopy (TEM) ex-situ measurements were also initiated using the JEOL 4000 with 1.4 A resolution and other high resolution microscopes in the Materials Science and Engineering Department of CWRU to study the molecular arrangement of transition metal phthalocyanines, particularly the sheet-polymeric phthalocyanines. TEM studies of adsorbed transition metal macrocycles on lacey carbon have indicated that the structure of the adsorbed layers is more complex than anticipated. Individual molecules are seen and clusters are evident under some circumstances. Special techniques are being developed which should facilitate the study of macrocycles on carbon and

graphite substrate including the HOPG. With the sheet-polymeric macrocycle we expect to establish whether the polymeric ligands are mostly in linear arrays or two-dimensional arrays.

In order to obtain further information concerning the redox behavior and O_2 reduction electrocatalytic properties of transition metal macrocycles, the effect of controlled poisoning by CO which competes with O_2 at the axial position of the transition metal in the macrocycle was examined. From the effects of CO on O_2 reduction electrocatalysis by transition metal macrocycles, it may be possible to examine if CO produced in-situ during carbon oxidation may degrade the O_2 reduction performance during fuel cell operation. Although CO is known to have significant poisoning effect in hemoglobin and other biologically important complexes, to our surprise the preliminary results in our laboratory have shown no substantial effects of CO on the redox behavior of FeTsPc adsorbed at a monolayer level on OPG in acid and alkaline solutions. Further studies are in progress.

2. **Polymer-modified electrodes**

Poly(4-vinyl pyridine) (PVP)-modified OPG electrodes with adsorbed CoTsPc exhibited much higher catalytic activity for O_2 reduction than the OPG electrode with only adsorbed CoTsPc in acid solutions. This may be due to the formation of an adduct between PVP and CoTsPc which is more active and more stable than the CoTsPc. However, a similar PVP-modified electrode exhibited inhibition for O_2 reduction in neutral and alkaline electrolytes.

PVP forms a protonated porous conducting film on the OPG electrode surface in acid solutions where the permeability of O_2 through the films is large. In neutral and alakline solutions the PVP film forms an unprotonated poorly conducting film on the OPG elctrode surface which considerably reduces the diffusion of O_2 through the film and increases the ohmic resistance. Over a

limited thickness range of the PVP (0.002 to 0.1 μm), there is practically no significant change in the catalytic activity for O_2 reduction in acid media.

3. **Transition metal oxide catalysts and bifunctional electrodes**

Anion-exchange membranes were found to greatly improve the performance of pyrochlore-based bifunctional oxygen electrodes when operating in the O_2 generation mode. This was believed to result partly from the membrane's ability to retard the transport of soluble Pb and Ru species out of the porous electrode. The heat-treated pyrochlores (~300°C) were much more corrosion-resistant.

The pyrochlore $Pb_2Ru_2O_{6.5}$ in self-supported, high-surface-area form is shown to have high activity for the 4-electron reduction of O_2 in alkaline solution. In gas-fed O_2 cathodes using a pore-former (ammonium bicarbonate), the cathodic performance in KOH was significantly better than that achieved with carbon supports. In the anodic mode, loss of the pyrochlore into the bulk electrolyte was a problem,. The application of an ionomer polymer layer to the solution side of the electrode did improve stability and activity in the anodic mode in KOH.

Several samples of lead ruthenates were prepared with various amounts of platinum substituted for the ruthenium. No significant gain in performance for O_2 reduction was found for the Pt-substituted lead ruthenates as compared to the lead ruthenate without Pt substitution. The Pt material was amorphous. Some samples of $Pb_2Ir_2O_{7-y}$ were also prepared and will be tested shortly.

Ruthenium pyrochlores have been found to be very effective catalysts for both O_2 reduction and generation. A series of ruthenium perovskites with the general formula $SrFe_xRu_{1-x}O_3$ has been synthesized following the nitrate decomposition method at 500°C to see if they can also serve as good bifunctional electrode catalysts. X-ray diffraction showed the presence of single-phase perovskites. Porous gas-fed electrode measurements on these perovskites in

alkaline solution showed less activity for both O_2 reduction and generation as compared to the ruthenium pyrochlores. The BET surface area, XPS, magnetic susceptibility, Mossbauer effect spectroscopy and hydrogen peroxide decomposition kinetic studies are being carried out to explore this difference.

Lithiated NiO is being examined as a catalyst for O_2 reduction and generation at ~200°C in concentrated KOH. At this temperature, the O_2 kinetics become essentially reversible at low currents. The research is designed to establish what changes in the electronic, magnetic and lattice properties of the NiO(Li) are responsible for the large increase in catalytic activity at temperatures approaching 200°C. At lower temperatures, (<150°C), NiO(Li) is a poor catalytic surface for reduction processes such as O_2 reduction which requires n-type rather than p-type semiconductors.

4. **Catalyst supports**

The use of mildly fluorinated carbon blacks as catalyst supports for platinum was explored in cooperation with the Electrosynthesis Company (ESC). Pt was deposited on the fluorinated and non-fluorinated carbons and the catalyst then examined using TEM and gas-fed electrode measurements at CWRU. The Pt dispersions in most cases for the fluorinated carbons, showed some non-uniformity and slightly larger particle sizes in comparison to that obtained for the non-fluorinated carbons. The O_2 reduction performance in 85% H_3PO_4 at 100°C was slightly poorer in most cases for the gas-fed electrodes made from the fluorinated carbons. The slightly higher polarization with the fluorinated carbon may reflect to the fact that the formulation and preparation of the porous gas-fed test electrodes were not yet optimized for this type of catalyst/support systems.

5. **The research during the subcontract year 1 April 1990 to 31 March 1991 will include:**

- structural studies of adsorbed macrocycle catalysts using STM, high resolution TEM, diffuse reflectance FT infrared, Raman (SERS and RR) and Mossbauer spectroscopy - (in-situ);
- effect of coordinating agents which compete for O_2 for the axial sites of the transiton metal in macrocycles for O_2 reduction;
- evaluation of electrochemical properties of polymer-modified electrodes;
- O_2 reduction and generation on transition metal oxides particularly the lithiated NiO at temperatures > 150°C;
- alternative and modified catalyst supports.

II. OBJECTIVES

The overall objectives of the research are

1. to develop a detailed understanding of the factors controlling O_2 reduction and generation on various electrocatalysts, including transition metal macrocycles and a number of types of oxide systems;
2. to use this understanding to identify and develop much higher activity catalysts, both monofunctional and bifunctional;
3. to establish how catalytic activity for a given O_2 electrocatalyst depends on catalyst-support interactions and to identify stable catalyst supports for bifunctional O_2 electrodes.

III. INTRODUCTION

Over the past two decades a large research effort has been carried out on a wide range of catalysts for O_2 reduction in alkaline and acid electrolytes and to a lesser extent on O_2 generation, principally in alkaline electrolytes. Much of this prior research by various groups has been semi-edisonian and lacked an adequate understanding of the electronic and steric factors

controlling the electrocatalytic activity. Consequently, the emphasis on O_2 electrocatalytic research at CWRU is on achieving a new level of understanding for both O_2 reduction and generation in relation to the basic properties of the catalyst-electrolyte interface. The research also is concerned with the failure mode involved with these catalysts.

Research during the past year at CWRU involved work principally on the following aspects of the catalyst systems:

A. Electrochemical and spectroscopic studies of the transition metal macrocycle catalysts.

B. Scanning tunneling microscope (STM) and high-resolution transmission electron microscope (TEM) studies of monomeric and sheet-polymeric macrocycle catalysts (ex-situ).

C. Adsorbed layers of dimeric macroycles designed to test the "dry cave" concept in O_2 electrocatalysis.

D. Controlled poisoning of transition metal macrocyles.

E. Polymer-modified electrodes: use of electronically conducting polymers as substrates for the adsorption attachment of transition metals.

F. Transition metal oxide catalysts including NiO(Li).

G. Bifunctional electrodes: Electrocatalytic aspects.

H. Catalyst supports for bifunctional electrodes.

IV. ACCOMPLISHMENTS DURING 1989-90.

A. Electrochemical and spectroscopic studies of the transition metal macrocycle catalysts.

Iron and cobalt tetrasulfonated phthalocyanines (TsPc's) were found in this laboratory to be good catalysts for O_2 reduction. The adsorption of iron and cobalt TsPc's was studied on several electrode surfaces including ordinary pyrolytic graphite (OPG) (1-5) and polycrystalline, as well as single-crystal

silver electrdes (6-7). The factors which affect the adsorption and particularly the orientation of the adsorbed complex are not fully understood. CoTsPc is readily adsorbed on OPG from aqueous solutions (acid, neutral and alkaline), while FeTsPc is adsorbed only from acid solutions and not from pure water or alkaline solutions (as is discussed later). In the present study the objective has been to develop an understanding of the factors influencing the adsorption of these complexes on graphite and metal electrodes. The charge under the voltammtric peaks corresponding to changes in the valency state of the metal was used to determine the surface concentration.

A-1. Adsorption of the tetrasulfonated phthalocyanines on ordinary pyrolytic graphite substrate

Two conditions for the preparation of the adsorbed layers of the TsPc's on OPG surface from their aqueous solutions were examined.

Preparation Condition I:

The complex was applied to the polished electrode surface by dipping it for 15 min into an air-saturated aqueous solution of macrocycle (~1 x 10^{-4} M) with the electrode under open-circuit condition and at low rotation rate (~100 rpm). The electrode was then removed and washed with pure water. The electrode with the adsorbed layer was next inserted into a deaerated electrolyte solution for voltammetric studies.

Preparation Condition II:

The polished electrode was dipped into a deaerated solution containing ~2 x 10^{-5} M macrocycle plus 0.1 M NaOH and then the electrode was cycled within a specified potential range for ~30 min or holding the electrode at a particular potential, while rotating at ~100 rpm for 15 min. The electrode was then removed, washed thoroughly with pure water and then inserted in a fresh deaerated electrolyte solution not containing the macrocycle for voltammetric studies. The OPG electrode was polished each time before adsorption at any

fixed potential.

Zecevic et al. (3) obtained four well-defined voltammetic peaks for FeTsPc (Fig. 1) and three for CoTsPc (Fig. 2) in 0.05 M Na_2SO_4 (pH = 10.7) with OPG when the adsorption was carried out with potential cycling between +0.3 V to -0.8 V vs. SCE at scan rates of ~100 mV/s for 30 min. In this case the measurement and the adsorbing solutions were both the same and consisted of 0.05 M Na_2SO_4 (pH = 10.7) plus 10^{-5} M FeTsPc or 10^{-5} M CoTsPc saturated with N_2. The most cathodic peak(1) for both the adsorbed complexes is assigned to the reduction of the TsPc ligand. Peaks (2) and (3) in Fig. 1 are assigned to the redox couples Fe(II)/Fe(I) and Fe(III)/Fe(II) for the adsorbed FeTsPc and likewise peaks (2) and (3) in Fig. 2 correspond to Co(II)/Co(I) as well as Co(III)/Co(II) for the adsorbed CoTsPc. The assignment of most anodic peak(4) in Fig. 1 for adsorbed FeTsPc is controversial and corresponds to either oxidation of the ligand or the redox couple Fe(IV)/Fe(III) (3, 10).

In the present study attention has been focused on peak 2 or peak 3 for adsorbed FeTsPc and peak 2 for adsorbed CoTsPc since valency state changes of the transition metal ions are believed to be of central importance to the oxygen electrocatalysis. The charge under these redox peaks has been used for determination of surface concentration of the macrocycles.

Voltammetry under preparation condition I

From a freshly prepared ~10^{-4} M solution of CoTsPc in pure water, the adsorption of CoTsPc occurred readily on OPG as seen from the voltammetry of the adsorbed electrode in 0.1 M NaOH solution (Table I). Its adsorption was increased by about a factor of two when adsorbed from either 0.25 M H_2SO_4, $NaClO_4$ or NaOH but was practically independent of the anions or pH of the adsorbing solution. This increase in adsorption of CoTsPc in the presence of supporting electrolyte may be due to some extent to the neutralization of the

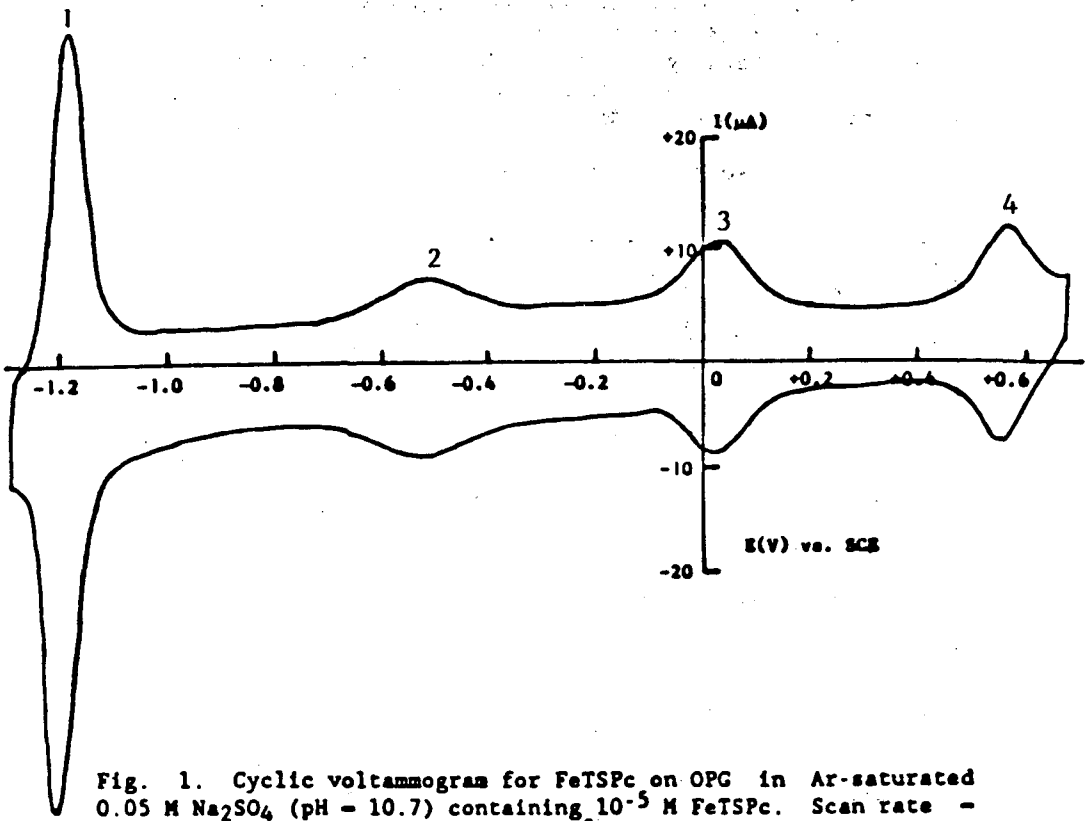

Fig. 1. Cyclic voltammogram for FeTSPc on OPG in Ar-saturated 0.05 M Na_2SO_4 (pH = 10.7) containing 10^{-5} M FeTSPc. Scan rate = 100 mV s^{-1}; electrode area = 0.2 cm^2; temperature = -23°C.

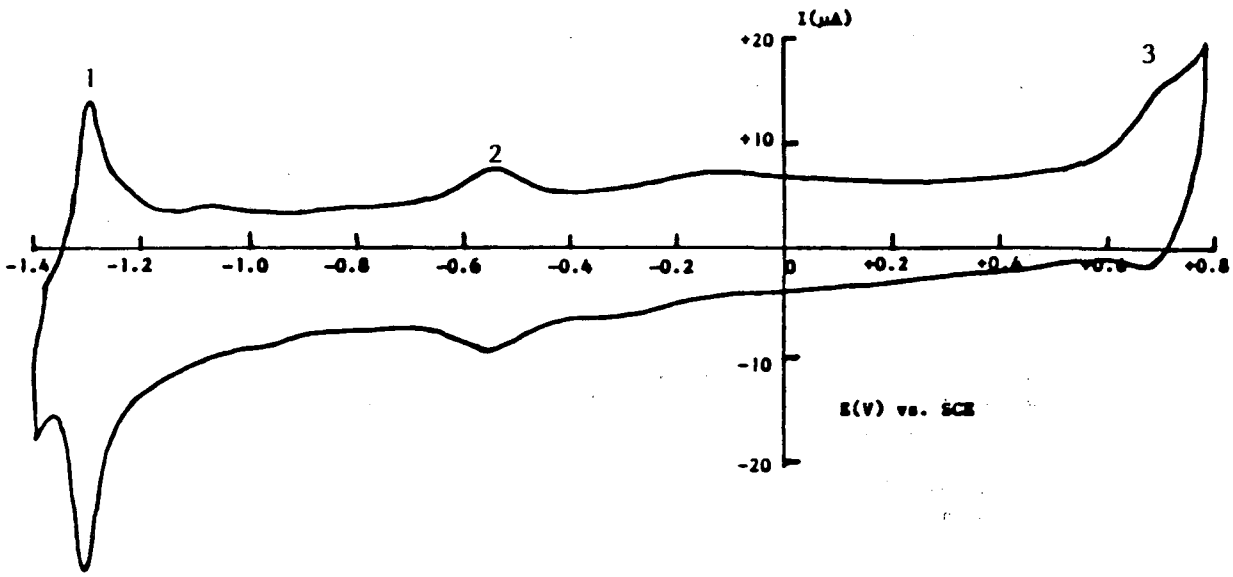

Fig. 2. Cyclic voltammogram for CoTSPc on OPG in Ar-saturated 0.05 M Na_2SO_4 (pH = 10.7) containing 10^{-5} M CoTSPc. Scan rate = 100 mV s^{-1}; electrode area = 0.2 cm^2; temperature = -23°C.

Table I. Voltammetry of CoTsPc adsorbed on OPG (preparation condition I) from acid, base and salt solutions containing ~10^{-4} M CoTsPc (measurement electrolyte = 0.1 M NaOH (Ar satd.), sweep rate = 150 mv/s and area of electrode = 0.2 cm^2)

Peak No.II: [Co(II)/Co(I)]

Adsorbing Solutions	E_m(V)	ΔE_p(V)	I_{pa}(μA)	Q(μC cm^{-2})	Moles cm^{-2}
H_2O	-0.525	0.020	0.60	2.60	2.9×10^{-11}
0.25 M H_2SO_4	-0.520	0.015	1.20	6.80	7.5×10^{-11}
0.5 M $HClO_4$	-0.525	0.010	1.10	5.86	6.5×10^{-11}
0.5 M $NaClO_4$	-0.530	0.010	0.95	5.54	6.1×10^{-11}
0.5 M NaOH	-0.520	0.005	1.10	5.68	6.3×10^{-11}

E_m = mean of anodic and cathodic peak potentials
ΔE_p = difference between anodic and cathodic peak potentials
I_{pa} = anodic peak current
Q = charge under the peak

Table II. Voltammetry of FeTsPc adsorbed on OPG (preparation condition I) from acid, base and salt solutions containing ~10^{-4} M FeTsPc (measurement electrolyte = 0.1 M NaOH (Ar satd.), sweep rate = 150 mv/s and area of electrode = 0.2 cm^{-2})

Peak No. III: [Fe(III)/Fe(II)]

Adsorbing Solutions	E_m(V)	DE_p(V)	I_{pa}(μA)	Q(μC cm^{-2})	Moles cm^{-2}
H_2O	-0.120	0.020	0.45	1.20	1.3×10^{-11}
0.5 M H_2SO_4	-0.125	0.010	1.60	6.80	7.5×10^{-11}
1.0 M $HClO_4$	-0.120	0.010	1.40	5.95	6.6×10^{-11}
1.0 M $NaClO_4$	-0.130	0.015	0.65	1.99	2.2×10^{-11}
1.0 M NaOH	-0.120	0.020	0.40	1.13	1.2×10^{-11}

E_m, ΔE_p, I_{pa} and Q as defined in Table I

Table III. Voltammetry for FeTsPc adsorbed on OPG under potential control (preparation condition II).
Adsorbing solution = ~2×10^{-5} M FeTsPc+0.1 M NaOH (Ar satd.).
Measurement solution = 0.1 M NaOH (Ar satd.).
Electrode area = 0.2 cm^2; Sweep rate = 150 mv/s.

Peak No. III [Fe(III)/Fe(II)]

Adsorbing Potentials	E_m(V)	ΔE_p(V)	I_{pa}(μA)	Q(μC cm^{-2})	Moles cm^{-2}
+0.100	-0.125	0.010	1.00	3.80	4.2×10^{-11}
-0.125	-0.120	0.005	1.05	4.37	4.8×10^{-11}
-0.300	-0.120	0.005	1.30	5.20	5.8×10^{-11}
-0.550	-0.120	0.000	2.20	9.53	10.6×10^{-11}
-0.750	-0.110	0.000	2.00	8.67	9.6×10^{-11}
-0.900	-0.095	0.010	1.40	5.60	6.2×10^{-11}

excess negative charge of the TsPc molecules by the cations of the electrolyte.

For FeTsPc, little adsorption was detected from a freshly prepared solution (~1 x 10^{-4} M) in pure water as indicated from the voltammetry of the adsorbed electrode in 0.1 M solution. It may be noted that the voltammetric peaks were not detected from FeTsPc solution in pure water if the solution was old even by 24 hours. This is consistent with the result reported by Elzing et al. [4] and shows that the FeTsPc transforms to a product [probably, $(FeTsPc)_2O$] which is not a favorable form for the adsorption. The little adsorption from freshly prepared solution may be due to the unchanged FeTsPc. The coverage is somewhat increased when the electrode was adsorbed from a solution of FeTsPc in 1 M $NaClO_4$ (see Table II) and was maximum for 1 M $HClO_4$ or 0.5 M H_2SO_4 adsorbing solutions. From the charge under the Fe(III)/Fe(II) peak (anodic sweep), the surface concentration was calculated and found to be ~7.5 x 10^{-11} moles/cm^2. This agrees reasonably well with that expected for compact monolayer (~8.0 x 10^{-11} moles/cm^2) assuming that the plane of the macrocycle ligand is parallel to the surface and occupies an area of ~2.0 nm^2 per molecule (1,5). The adsorption of FeTsPc from 1 M NaOH solution is not significantly different from that obtained in pure water (Table II). This indicates that the adsorption of FeTsPc, using preparation condition I, is primarily dependent on the pH of the adsorbing solution and the effect of ionic strength plays a secondary role.

Elzing et al. [4] found a similar increase in the height of the peaks 2 and 3 as measured in 1.0 M KOH, when $LiClO_4$, KOH or H_2SO_4 was added to the FeTsPc solution in pure water from which FeTsPc layer on pyrolytic graphite was formed. They reported that if the concentration of any of these electrolytes in the adsorbing solution was increased, then the coverage of FeTsPc was also increased and approached a limiting value at 1 M concentration for these electrolytes. In the present work the peaks were also higher for FeTsPc adsorbed

from more concentrated acid solutions and reached a limiting value at ~1 M concentration of the acid. The adsorption of FeTsPc on OPG from a solution of ~10^{-4} M FeTsPc in pure water or from 1.0 M NaOH was much less as compared to that in the presence of the same concentration of the acid (Table II). Similar adsorption behavior of FeTsPc was found using preparation condition I in 0.05 M H_2SO_4 as the measurement solution.

Voltammetry for electrode prepared with potential control (preparation condition II)

Well-defined voltammetric peaks were obtained by Zecevic et al. with the OPG substrate when the adsorption was carried out with potential cycling for about 30 min within a specified potential range (+0.3 to -0.8 V vs. SCE), and the adsorbing and measurement solutions were both the same and consisted of 0.05 M Na_2SO_4 (pH = 10.7) plus 10^{-5} M FeTsPc. Well-defined voltammetric peaks were also obtained when the adsorption was carried out under potential control. Table III gives the surface concentrations based on charge under peak 3 while FeTsPc was adsorbed from a deaerated solution containing 0.1 M NaOH plus ~2 x 10^{-5} M FeTsPc at various potentials for 15 min with the electrode rotating at ~100 rpm. The electrode with the adsorbed layer on it was then removed, washed with pure water and introduced into deaerated 0.1 M NaOH without the macrocycle in solution for voltammetric studies. The coverage was evaluated from the anodic peak corresponding to Fe(III)/Fe(II) for the adsorption potentials indicated in Table III. The maximum value of 1.06 x 10^{-10} moles/cm^2 was obtained for the electrode prepared at -0.55 V vs. SCE. This electrode did not show any change in the peak height after cycling the potential between +0.2 to -0.9 V continuously for 5 min. The amount that is adsorbed, however, does not depend significantly on the potential at which it was adsorbed, using the charge under anodic voltammetry peak 3 as indication of the amount adsorbed. FeTsPc was adsorbed on the electrode at either -1.4 V or +0.55 V (corresponding

to the potentials for peak 1 and peak 4 respectively in the voltammetry of adsorbed FeTsPc in 0.1 M NaOH). The peak heights were very small and additional new peaks appeared. This can be explained on the basis of the decomposition of the ligand (3).

In alkaline solutions containing FeTsPc (~2 x 10^{-5} M) the peak heights increased with time if the potential was cycled within a specified range (+0.2 to -0.9 V vs. SCE) and attained a steady-state coverage of ~3 x 10^{-11} moles/cm^2 in 0.1 M NaOH and ~4.7 x 10^{-11} moles/cm^2 in 1 M NaOH. In acid solutions, the maximum peak heights were attained immediately and then decreased to some extent with time before reaching the steady-state coverage under similar condition. The surface concentrations corresponding to the steady state were 5.5 x 10^{-11} moles/cm^2 in 0.05 M H_2SO_4 and 1.0 x 10^{-10} moles/cm^2 in 0.5 M H_2SO_4. This indicates the role of the ionic strength in the adsorption of FeTsPc on OPG.

FeTsPc adsorbed on an OPG elctrode by dipping it in an aqueous solution of 10^{-4} M FeTsPc in 0.5 M H_2SO_4 (preparation condition I) showed well-defined voltammetric peaks in deaerated 0.1 M NaOH. When the same electrode, after washing with pure water, was tested in deaerated 0.05 M H_2SO_4 solution, peaks 2 and 3 were suppressed. When this electrode, after the voltammetric run in 0.05 M H_2SO_4, was again run in 0.1 M NaOH, the peaks were greatly reduced in height. This indicated desorption or demetallation of FeTsPc from the surface. Adsorbed FeTsPc on OPG seems to be less stable in 0.05 M H_2SO_4 as compared to 0.1 M NaOH in voltammetric experiments under similar condition. The decrease in peak heights was also observed if the voltage window was opened to more cathodic values corresponding to peak 1 or more anodic values corresponding to peak 4 (see ref. 3).

Spectroscopic studies of tetrasulfonated phthalocyanines

Earlier in this report CoTsPc and FeTsPc adsorbed from their solutions in pure water were reported (preparation condition I) to differ greatly in the extent of their adsorption: Q(CoTsPc) > Q(FeTsPc) where Q is the charge under the peak. In order to gain more insight into their differences, uv-visible absorption spectroscopic studies were made for these compounds in the solution phase (0.1 M NaOH) with and without cyanide (1×10^{-3} M) which coordinates with the specific valency states of the transition metal such as Fe and Co in phthalocyanines and porphyrins.

The uv-visible absorption spectra of μ-oxo bis[tetra(dodecyl sulfonamido)-phthalocyanato-Fe(III)], $[TdPcFe(III)]_2O$ and its non-μ-oxo form have been reported in DMF solution by Lever et al. (9). The Q band of the μ-oxo species (633 nm) agreed well with the Q band of the FeTsPc in aqueous and/or 0.1 M NaOH solution (634 nm) obtained in our laboratory. This indicates that the FeTsPc in aqueous and/or alkaline solution may be present mostly in the μ-oxo, $(FeTsPc)_2O$ form since the Q band of the monomeric species [TdPcFe(II)] is at a longer wave length. These resuts are qualitative because the solvents used for the two measurements were different (e.g., NaOH solvent for FeTsPc and DMF for TdPcFe).

Additional evidence for the presence of the μ-oxo species of FeTsPc in alkaline solution is based on the fact that the spectra of FeTsPc in aqueous and/or 0.1 M NaOH are the same with and without CN^- in the solution (Fig. 3). Oxygen is strongly bound axially between the two irons in the μ-oxo-bridged dimer (Fe-O-Fe) and is not displaced by the CN^- ions (10). The interaction of CN^- ions with the opposite axial position would be expected to be quite weak in the μ-oxo complex. FTIR spectrum for the solid FeTsPc complex in KBr indicated that FeTsPc was unlikely to be present in the μ-oxo form in the solid phase (Fig. 4). Mossbauer spectra of the solid FeTsPc complex also indicated that it

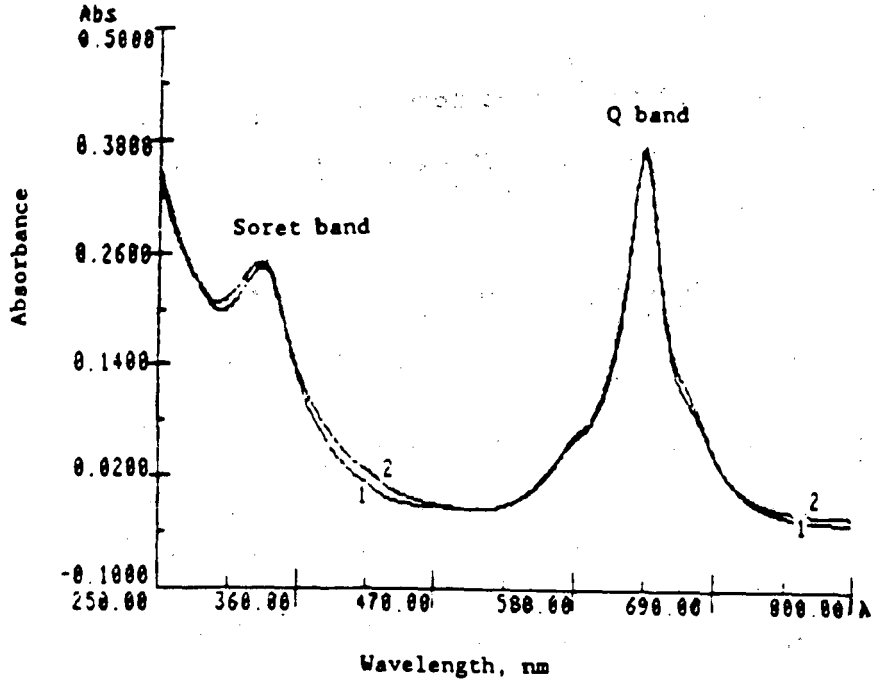

Fig. 3. Uv-visible absorption spectra for 10^{-5} FeTSPc in 0.1 M NaOH without (1) and with (2) 10^{-3} CN^- in solution. Path length = 1.0 cm.

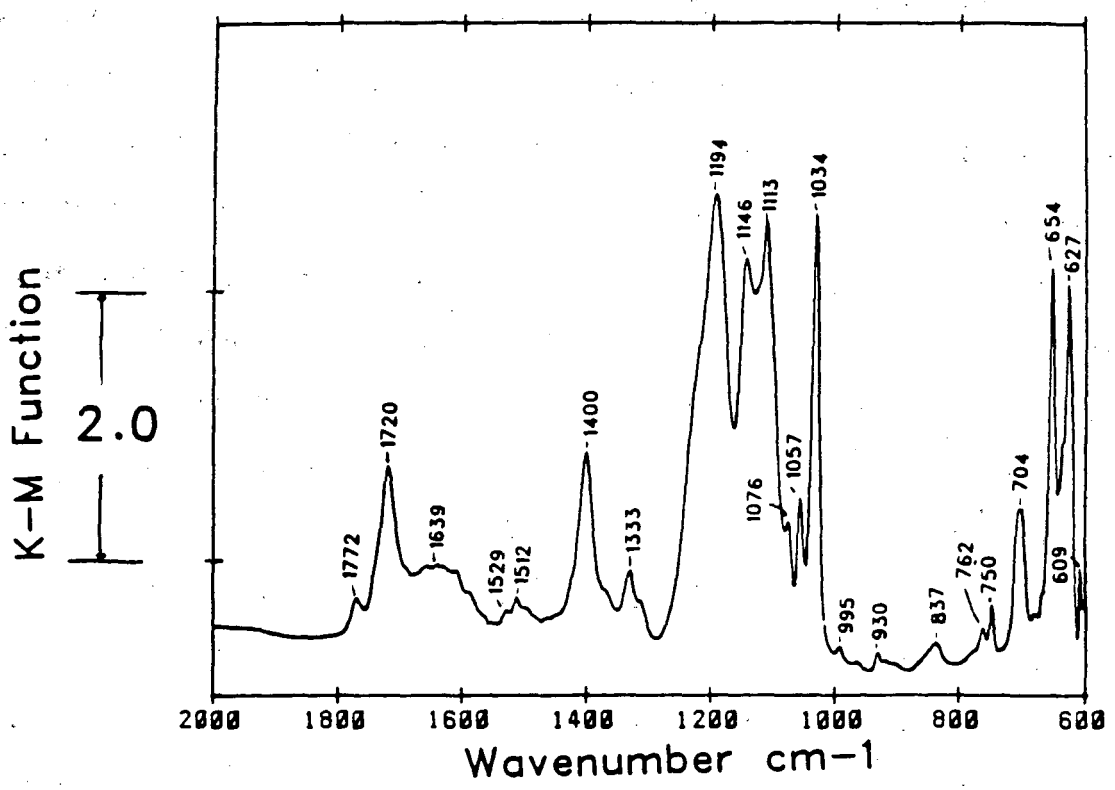

Fig. 4. Diffuse reflectance FTIR spectrum of FeTsPc in KBr. The K-M function = $(1-R)^2/2R$, where R is the reflectance.

was present mostly in the FeTsPc form although there were indications that the complex adsorbed on Vulcan XC-72 carbon from aqueous solution was in the μ-oxo form (11).

In strong acid solutions FeTsPc is present mostly in the monomeric form. The absorption spectrum of FeTsPc in 0.5 M H_2SO_4 is somewhat different from that in 0.1 M NaOH, particularly in the Soret band (Fig. 5). The differences in the adsorption behavior of FeTsPc and CoTsPc from their aqueous solutions in presence of air are related to the structural differences of the two complexes in solution and their binding to the graphite surface.

A-2. Adsorption of tetrasulfonated phthalocyanines on highly ordered pyrolytic graphite (HOPG)

In order to gain more insight into the orientation of water-soluble tetrasulfonated phthalocyanines on smooth substrate, the adsorption of these compounds was examined on HOPG. The background voltammogram for the basal plane of a freshly peeled HOPG (Union Carbide) in N_2-purged 0.05 M H_2SO_4 showed a good potential window, -0.4 to 1.0 V vs. SCE. The double layer capacitance at 0.0 V from the voltammetric curve at 100mV/s was 3.2 $\mu F/cm^2$ which agrees well with the value obtained by Randin et al. (12). CoTsPc showed adsorption from well-deaerated solution in 0.05 M H_2SO_4 while FeTsPc showed very slow adsorption under similar conditions of potential control. However, introduction of O_2 in the deaerated FeTsPc solution in 0.05 M H_2SO_4 accelerated the adsorption of FeTsPc on the HOPG surface. (Fig. 6).

The assignments for the peaks are similar to the voltammetry of the adsorbed macrocycles on the ordinary pyrolytic graphite (OPG) surface. The peak separations between anodic and cathodic peaks at a scan rate of 500 mV/s are close to 0.0 V, which indicates fast charge transfer rates. The coverages calculated from the charge under the peaks (anodic) were 2.9×10^{-11} and 3.5×10^{-11} moles/cm^2 for CoTsPc and FeTsPc, respectively. The slightly higher value

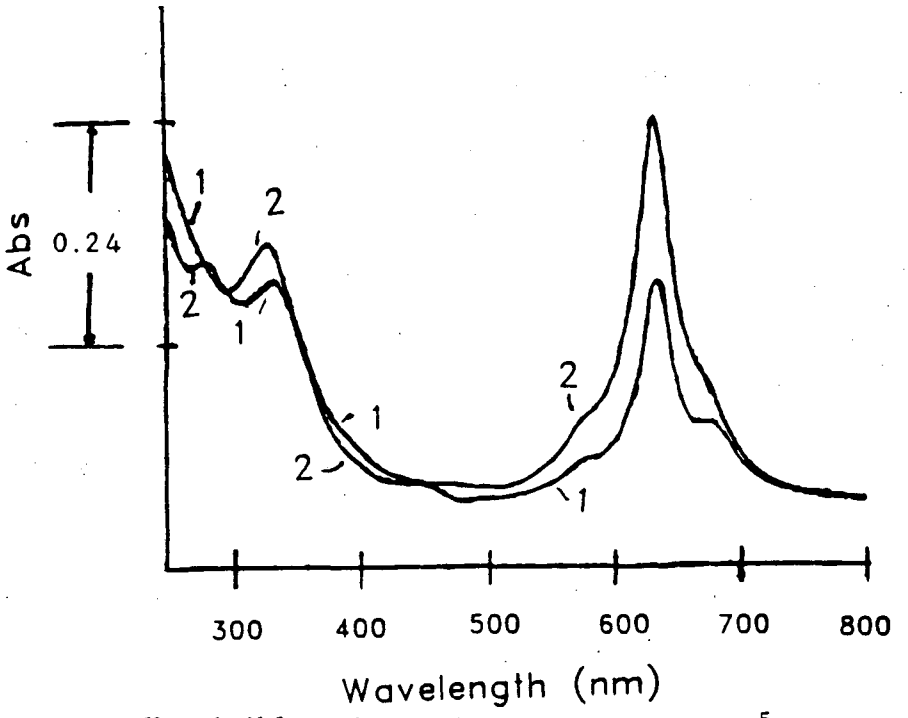

Fig. 5. Uv-visible absorption spectra for 10^{-5} M FeTsPc in 0.5 M H_2SO_4 (1) and 0.1 M NaOH (2). Path length = 1.0 cm.

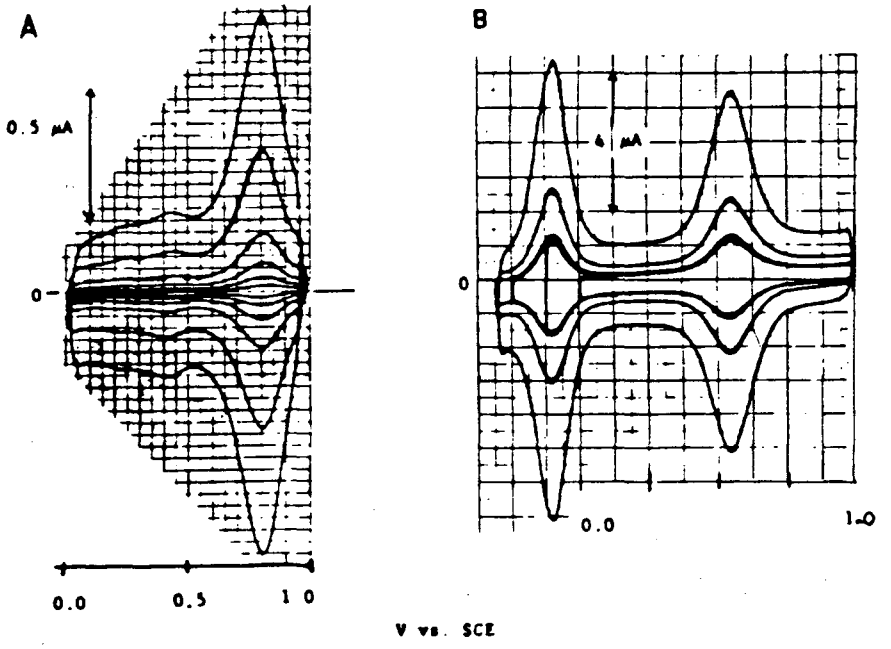

Fig. 6 Cyclic voltammograms for transition metal macrocycles adsorbed on the basal plane of HOPH, without macrocycle present in the argon-saturated 0.05 M H_2SO_4: (A) CoTSPc at a coverage of 2.9×10^{-11} mol cm^{-2}, with sweep rates 20, 50, 100, 200, 500 and 1000 mV s^{-1} (electrode area = 0.45 cm^2); (B) FeTSPc at a coverage of 3.5×10^{-11} mol cm^{-2}, with sweep rates 100, 200 and 500 mV s^{-1} (electrode area = 0.32 cm^2).

for FeTsPc may be due to the defects produced during the peeling procedure since the double layer capacitance is slightly higher than that in the CoTsPc case. The molecular planar area calculated for these compounds is ~260 $Å^2$. If all of the molecules are parallel and compactly adsorbed on HOPG, the surface concentration would be 6 x 10^{-11} moles/cm^2 which is almost twice the experimental values.

A-3. Adsorption of tetrasulfonated phthalocyanines on Pt and Au surfaces

When FeTsPc was injected into the cell during potential cycling (-0.27 to 0.40 V vs. SCE) of a Pt electrode in 0.1 M $HClO_4$, the hydrogen adsorption and the double layer capacitance decreased which supports the adsorption of FeTsPc on Pt (Fig. 7). The FeTsPc was not adsorbed when the potential was swept into the Pt anodic film region. The current during the anodic sweep through the hydrogen region exceeded the oxidation current for the bare electrode. The difference in the calculated charge for hydrogen adsorption in the absence and in the presence of FeTsPc on the surface indicated that ~40% of the Pt surface is still available for hydrogen adsorption at the saturation coverage of FeTsPc. This is in agreement with the STM images obtained by Lippel et al. (13) which show significant intermolecular void spaces at one monolayer coverage.

A gold electrode prepared by vapor deposition was tested in the Au double layer region (-0.40 to +1.0 V in 0.1 M $HClO_4$) for adsorption of these compounds in the same fashion but no evidence for adsorption was found. When the limit for the anodic sweep was opened up to 1.30 V vs. SCE in 0.1 M $HClO_4$, a pair of oxidation reduction peaks were observed at -0.2 V and remained even after the solution was replaced with fresh electrolyte solution free of CoTsPc. These voltammetric peaks were stable during potential cycling into the Au oxide region, but disappeared upon sweeping the potential to hydrogen evolution.

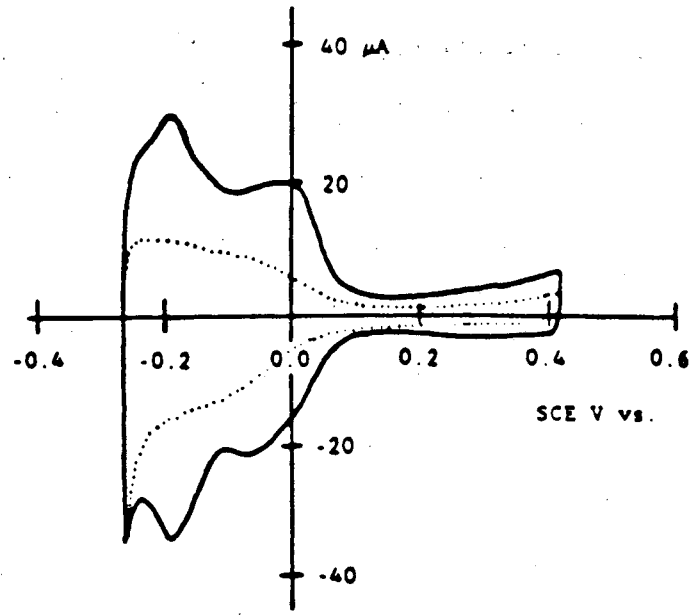

Fig. 7. Cyclic voltammetry curves for a Pt electrode in argon-saturated 0.1 M $HClO_4$: (····) with adsorbed FeTSPc (none present in the solution); (——) with no adsorbed macrocycle. Electrode area = 0.2 cm^2; sweep rate = 100 mV s^{-1}.

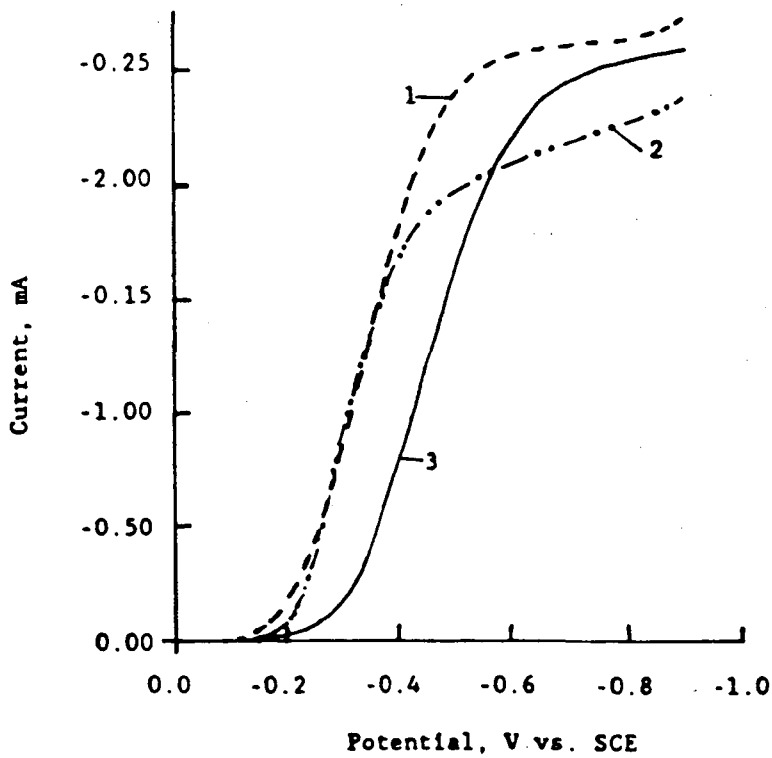

Fig 8. Rotating disk electrode polarization curves for O_2 reduction on silver: 1) with adsorbed FeTSPc; 2) with adsorbed CoTSPc; and 3) without adsorbed macrocycle. Electrolyte = O_2-saturated (1 atm) 0.1 M NaOH; electrode area = 0.45 cm^2; scan rate = 10 mV s^{-1}; rotation rate = 2500 rpm.

This pair of peaks appears to correspond to ligand reduction/oxidation. The same features were observed for FeTsPc. No adsorption of these TsPc complexes was observed on the gold surfaces. The reason for this is under investigation.

A-4. Cyclic voltammetry and O_2 electrocatalytic studies of tetrasulfonated phthalocyanines adsorbed on polycrystalline Ag in acid and alkaline solutions

Much work has been done in this laboratory on the adsorption of FeTsPc and CoTsPc on polycrystalline as well as single crystal Ag, including the Raman spectroscopy (SERS and Resonant Raman). Still questions remain unanswered, particularly regarding the orientation of the macrocyclic films on Ag at monolayer coverages. The work during the past year involved the adsorption of FeTsPc and CoTsPc on mechanically polished polycrystalline Ag electrode to obtain the maximum coverage corresponding to a monolayer and the O_2 reduction kinetics on such macrocycles, adsorbed on Ag electrodes in acid and alkaline electrolytes.

The adsorption of TsPc's on Ag depends on the pH of the solution, the nature of the electrode surface and potential cycling. There were well-defined voltammetric peaks in acid solution (0.05 M H_2SO_4) whereas no peaks were observed in alkaline solution (0.1 M NaOH). The height of the peaks increased and attained a constant value after potential cycling (+0.1 to -0.6 V vs. SCE) for about 30 min. The structure of the adsorbed layer is quite different in acid and alkaline electrolytes. FeTsPc generally gives four well-defined peaks on OPG substrate depending on the pH of the solution. Only two peaks rather than four were observed on Ag in 0.05 M H_2SO_4 because Ag is oxidized at relatively low positive potentials. The charge associated with the most cathodic peak assigned to the ligand reduction (peak 1) was much higher than the less cathodic peak (peak 2) in agreement with the earlier results in this laboratory (7).

No catalytic activity for O_2 reduction was found for FeTsPc or CoTsPc

adsorbed on Ag electrodes in 0.05 M H_2SO_4. The O_2 reduction polarization is reduced by ~100 mV with CoTsPc or FeTsPc adsorbed on Ag electrodes in 0.1 M NaOH (Fig. 8). The voltammetry of adsorbed FeTsPc on Ag in 0.1 M NaOH showed a distinct cathodic and anodic irreversible pair of peaks when the electrode was scanned to more cathodic potentials (~-1.2 V vs. SCE) (Fig. 9). No such peaks were observed in the voltammetry of adsorbed CoTsPc on Ag under similar conditions. The assignment of the irreversible peaks associated with adsorbed FeTsPc on Ag in 0.1 M NaOH when the electrode is scanned to higher cathodic potentials is under study.

These studies reveal that the adsaOH when the electrode is scanned to higher cathodic potentials is under study.

These studies reveal that the adsorption and retention of the macrocycle complexes on electrode surfaces are quite complex phenomena and depend in a rather elaborate manner on the prevailing conditions. In-situ optical spectroscopic techniques and STM are promising means for monitoring surface changes in the adsorbed layer as well as the substrate.

B. STM and high resolution TEM studies of monomeric and sheet-polymeric phthalocyanines

Of special interest in learning the mechanism for the O_2 reduction on macrocycles is the comparison of the mechanism and kinetics on CoPc and FePc and the corresponding sheet-type polymers $(CoPc)_x$ and $(FePc)_x$. Both the monomer and sheet polymer of FePc catalyze the $4e^-$ reduction of O_2 to OH^-. The peroxide bridge model, (M-O-O-M), for the adsorbed FePc monomer has been proposed to explain the 4-electron reduction. Such a mechanism is much less likely with the adsorbed $(FePc)_x$ polymer since the latter is expected to be parallel to the surface. One complication is that the configuration of the sheet polymer and even its molecular weight are uncertain. Thus it is not known reliably whether the sheet polymer is a one-dimensional linear array or a

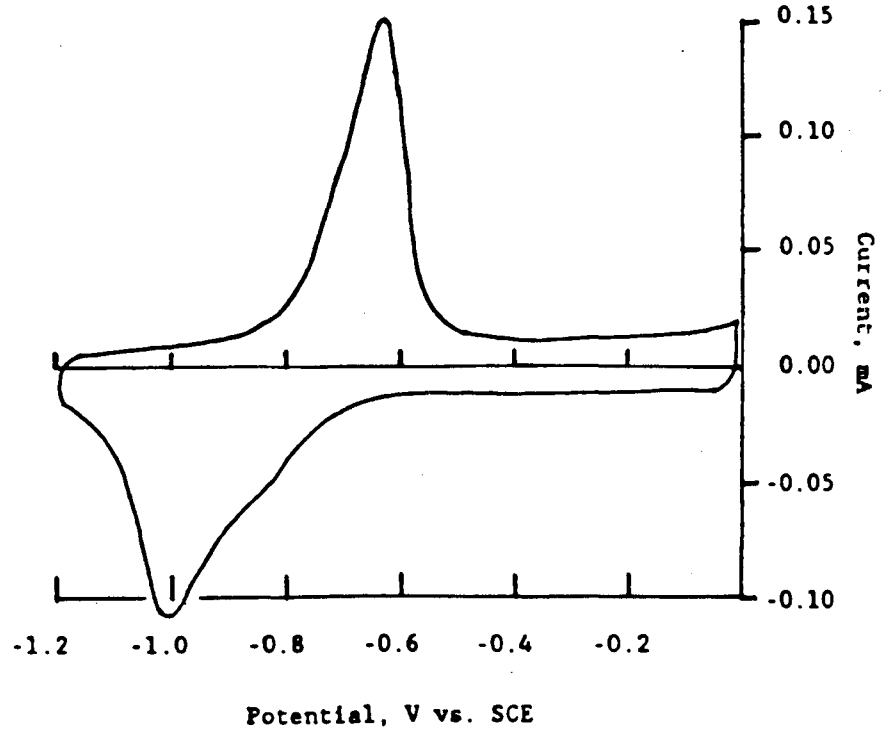

Fig. 9. Cyclic voltammogram of an adsorbed layer of FeTSPc on a polycystalline silver electrode in Ar-saturated 0.1 M NaOH. Electrode area = 0.45 cm^2; scan rate = 150 mV s^{-1}.

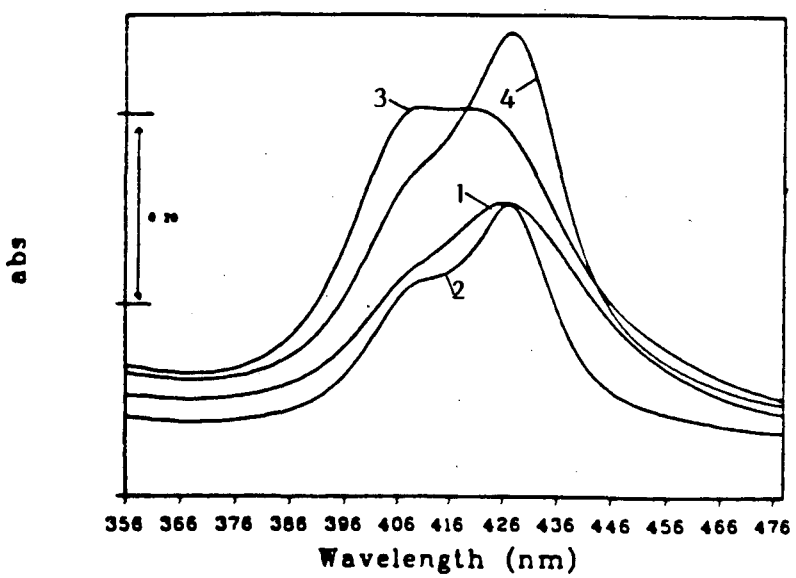

Fig. 10. Uv-visible absorption spectra (Soret band) for cationic and anionic porphyrins and the ion-paired dimer in 1:1 water-acetone (v/v): 1) 1 x 10^{-5} M CoTTAPP (cation); 2) 1 x 10^{-5} M CoTSPP (anion); 3) 1 x 10^{-5} M CoTTAPP and CoTSPP; 4) 1 x 10^{-6} M CoTTAPP and CoTSPP. A 1.0 cm path length cell was used for 1, 2 and 3, while a 0.1 cm cell was used for 4.

two-dimensional array approximating a square configuration. STM and TEM can provide such information but only STM can do so in-situ.

So far only preliminary studies have been carried out for the polymer using STM and TEM at CWRU. Critical results are expected to be obtained shortly. Polymeric CuPc, FePc and CoPc were synthesized and purified following the method of Achar et al. (14) and characterized using uv-visible spectroscopy and cyclic voltammetry.

B-1. Scanning tunneling microscopic (STM) studies

Research was initiated with STM on macrocycles (CoTsPc) adsorbed on HOPG at monolayer and submonolayer concentrations. A Nanoscope I (Digital Instruments) was initially used for the preliminary ex-situ measurements. While the HOPG substrate was visible at atomic levels, the CoTsPc layer was not. Consequently the visualization of this macrocycle complex adsorbed on HOPG was attempted with the Nanoscope II in the B.P. America laboratories in Cleveland. This instrument has image enhancement software. The research effort on the STM studies of the transition metal complexes was quite restricted initially but will be considerably increased as we have recently received our own Nanoscope II from Digital Instruments, Inc.

Lippel et al. (13) have reported micrographs of copper phthalocyanine (CuPc) adsorbed on Cu(100) in an ultra high vacuum chamber at room temperature. The electron density obtained from Huckel molecular orbital calculations was ideally matched to the experimental images. Additionally, the orientation of the CuPC was with the macrocycle ligand parallel to the surface, which was attributed to the strong Cu-Cu adsorbate-substrate interaction (14). However, the same orientation need not prevail under electrochemical conditions. In-situ STM measurements are needed to examine this question.

In further efforts to image the monolayer adsorbed phthalocyanines,

including the sheet-type polymeric phthalocyanines, on highly ordered pyrolytic graphite (HOPG), the Nanoscope II at BP America was used ex-situ to study the structure of polymeric Cu-phthalocyanine adsorbed on HOPG. The polymeric CuPc was applied to the HOPG surface from a drop of solution and the solvent evaporated. Crystallites were observed with STM.

B-2. High-resolution TEM studies

High-resolution electron microscopy can be used to analyze the molecular arrangements in thin films (see ref. 18). In collaboration with Dr. P. Pirouz of the Materials Science and Engineering Department of CWRU, work has been initiated with high-resolution (~1.35 Å) TEM (JOEL 4000) to study the molecular structure of adsorbed transition metal phthalocyanines, particularly the polymeric phthalocyanines. TEM specimens were prepared by supporting samples on a holey carbon film (Ted-Pella Inc., Redding, CA). The electron diffraction patterns of the supported film can yield information concerning the structure of the film including the orientation of the macrocycle species.

Recent studies of transition metal macrocycle crystallites on lacey carbon by TEM have indicated that the structure of the crystallites is more complex than anticipated. Individual molecules and clusters are evident under some circumstances. With HOPG as the substrate, the challenge is to achieve a sufficiently thin substrate for the adsorbed $(FePc)_x$ to be discernable. One way of achieving sufficient contrast is to bind a heavy metal species to the acid groups along the periphery of the polymeric sheets. Another approach is to intercalate the HOPG with a mixture of oxidizing acids, thus defoliating the HOPG into very thin sheets, as done in the manufacture of Grafoil from naturally occurring single crystal graphite and then to use these very thin graphite sheets as the substrate.

C. Adsorbed layers of dimeric macrocycles designed to test the "dry cave" concept

During the past year, work was initiated on adsorbed layers of dimeric macrocycles designed to test the "dry cave" concept. An approach was initiated at CWRU for the preparation of 'sandwich-type' binuclear transition metal macrocycles on OPG surface. This is based on the work of Linschitz and co-workers (15) who have examined such diporphyrins in solution spectroscopically. Their approach involved the spontaneous association of the two macrocycles in solution, one with cationic charge on the macrocycle ligand and the other with anionic charge, using either water or ethanol as the solvent. With the charged groups attached to the benezene ring of the transition metal macrocycles, sandwich structures are formed with the two macrocycles parallel to each other and a cavity between them. This cavity provides a hydrophobic environment and is expected to increase the rate of adsorption of O_2 at the coordination sites of the transition metal in the macrocycle complex.

Positively charged tetra kis(4-trimethyl ammonium phenyl) porphyrin (TTAPP) and negatively charged tetra kis(sulfonated phenyl) porphyrin (TSPP) with cobalt ion as the metal center were synthesized and characterized by uv-visible and diffuse reflectance FTIR spectroscopy. Mixtures of the aqueous solutions of the two oppositely charged porphyrins gave a precipitate which was also characterized by the same spectroscopic techniques after the product was washed and dried. The product was then dissolved in a 1:1 acetone water solution and the uv-visible spectra determined. This spectrum was essentially the same as that for the mixture of TTAPP and TSPP in the same solvent but differed from that of the individual components in the same solvent (Fig. 10). Diffuse reflectance FTIR spectra for the solid monomers and dimer in a KBr matrix under N_2 atmosphere were also obtained (Fig. 11). FTIR measurements are in progress with these species in solution. The spectral features for the

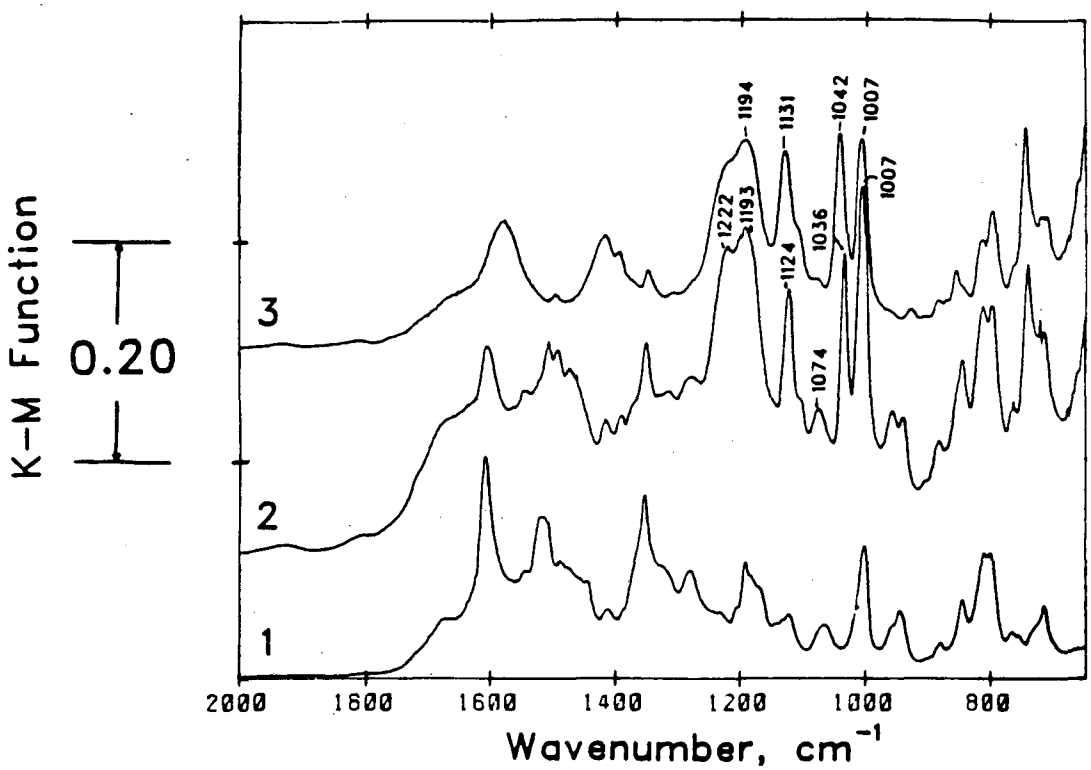

Fig. 11. Diffuse reflectance FTIR spectra of 1, CoTTAPP, 2 wt% in KBr; 2, CoDIMER, 4 wt% in KBr and 3, CoTSPP, 2 wt% in KBr. (CoDIMER is the complex between CoTTAPP and CoTSPP isolated from aqueous solution.)

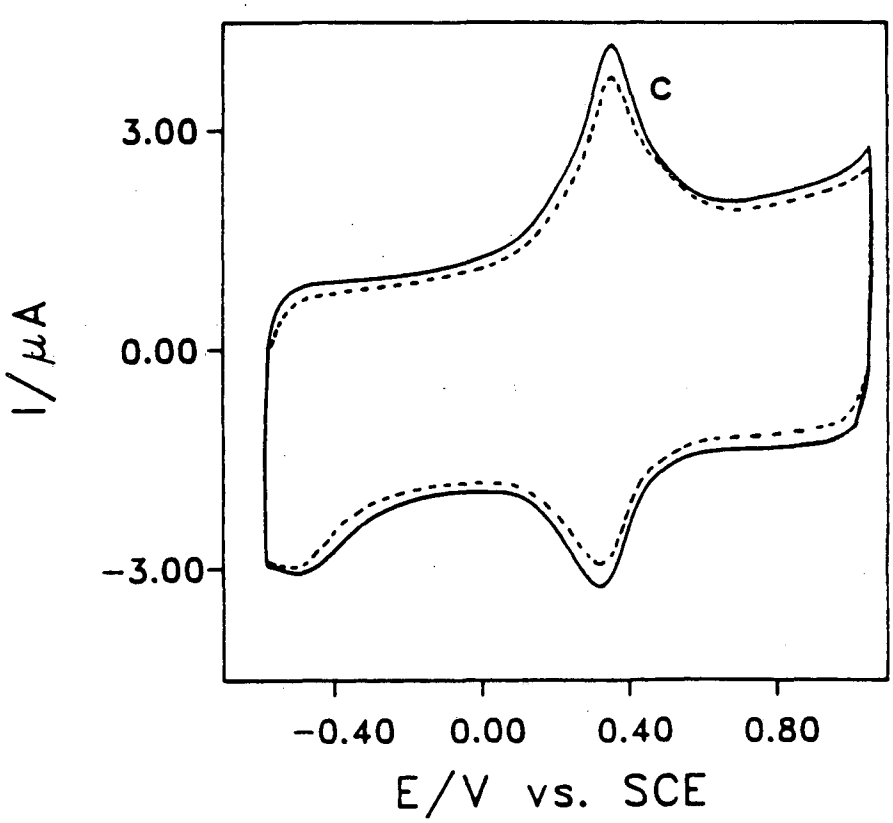

Fig. 12. Cyclic voltammograms on OPG (----) and OPG/PVP (——) electrodes in N_2-saturated 0.05 M H_2SO_4 solutions. Scan rate = 200 mV/s.

sulfonic groups in the monomer and dimer were quite different. This indicates an interaction between the macrocyles through sulfonic and ammonium-phenyl groups.

Cyclic voltammetry and O_2 reduction electrocatalytic activity for the TTAPP and TSPP monomers and their dimer adsorbed on HOPG surface are under investigation.

D. Controlled poisoning of transition metal macrocycles by CO

In order to obtain further information concerning the redox properties and O_2 reduction electrocatalysis on transition metal macrocycles, the effect of controlled poisoning by CO which competes with O_2 at the axial position of the transition metal in the macrocycle was examined. From the effects of CO on O_2 reduction electrocatalysis on transition metal macrocycles, it may be possible to examine if CO produced <u>in-situ</u> during carbon oxidation may degrade the O_2 reduction performance during fuel cell operation. Earlier results (10) in this laboratory have shown that CN^- ions coordinate with specific valency states of the transition metals such as Fe and Co in phthalocyanines and porphyrins and has substantial poisoning effect on O_2 reduction. Although CO is known to have significant poisoning effect in hemoglobin and other biologically important complexes, to our surprise the preliminary results in our laboratory showed no substantial effect of CO on the redox behavior of iron tetrasulfonated phthalocyanine adsorbed at monolayer level on ordinary pyrolytic graphite (OPG) electrode in acid and alkaline electrolytes. Further studies are in progress to examine the effect of CO on the electrocatalytic properties of adsorbed Fe-TsPc and CoTsPc as well as Fe- and Co-porphyrins for O_2 reduction.

E. Polymer-modified electrodes

Ionically conductive polymers have been considered both as replacements for the electrolyte within the porous layer of gas-fed electrodes and also as an additional outer ionically conducting layer. The use of Nafion as an over-

layer on electrode surfaces was proposed by the CWRU group to inhibit the loss of the transition metal and/or the complex as a whole into the bulk of the electrolyte solution. The replacement of the fluid electrolytic solution with a conducting perfluoro-ionomer is attractive because of the much higher solubility of O_2 in the polymer. With Nafion as the ionomer, the polymer usually is considered to consist of a continuous hydrophobic phase and a dispersed hydrophillic phase and this may help facilitate the adsorption of the non-polar O_2 molecules in competition with much more polar species such as H_2O and H_xPO_4 species on the transition metal sites (i.e., the "dry cave" effect). This effect is expected to be most pronounced on the electrode surface when the continuous hydrophobic phase is in contact with the catalyst sites but some beneficial effect is to be expected even at catalyst sites which are in contact with the more hydrophillic dispersed phase. The use of a polymer as the ionic conducting electrolytic solution should also prove attractive for long life since it immobilizes the ionic conducting solution within the porous gas-fed electrode and hence prevents redistribution of the electrolyte phase within the porous electrode. The polymer also facilitates the operation of the porous gas-fed electrodes as well as gas-generating electrodes with substantial pressure differentials between the solution and gas phases.

Measurements have been carried out at CWRU, which in good part verify these predictions. The research has involved both smooth electrode surfaces (OPG, Pt, Au) and high area gas-fed porous carbon electrodes with CoTMPP (with and without heat treatment) and also highly dispersed Pt catalysts. With smooth OPG electrode surfaces, it has been found necessary to have CoTsPc added also to the Nafion phase in order to achieve the enhancement. This may be caused by the tendency of CoTsPc to desorb into the polymer solution phase during the application of the polymer to the OPG substrate.

The research during the past year has included the basic research on the PVP-modified ordinary pyrolytic graphite (OPG) electrodes with adsorbed cobalt tetrasulfonated phthalocyanine (CoTsPc) for O_2 reduction in acid electrolytes. Such electrodes have been characterized by linear sweep voltammetry. The influence of thickness of the PVP film, pH of the electrolyte and the method of preparation of the modified electrodes have been investigate for O_2 reduction activity. Adducts formed between PVP and CoTsPc have been isolated from acid and neutral solutions and examined for their activity for O_2 reduction. FTIR and uv-vsible spectroscopic techniques have been used to identify the adducts.

Isolation of PVP-CoTsPc adducts from the solution

Adduct I was obtained by mixing 13 ml of 1.2 mg/ml PVP solution in pure methanol with 2 ml of 10 mg/ml CoTsPc solution in pure water. After the mixture was kept at 60°C for 5 h, the solvent was removed, and the solid was vacuum dried at 60°C overnight. It was washed with pure water and methanol, and finally dried under vacuum at 60°C overnight.

Adduct II was obtained by mixing 3 ml of 3.3 mg/ml PVP solution in pure methanol and 15 ml of 1 mg/ml CoTsPc solution in 0.05 M H_2SO_4. The dark blue precipitate appeared immediately after mixing, which was filtered and washed with pure water and methanol and dried in vacuum at 50°C overnight.

Preparation of modified electrodes

The modified electrodes were prepared in three different ways:

(1) OPG/CoTsPc/PVP

The OPG electrode was immersed in 1 x 10^{-4} M CoTsPc in air-saturated water for 15 min without potential control with the electrode rotating at ~30 rpm. The electrode was removed and washed with distilled water. It was then immersed in a PVP solution (8 x 10^{-4} mg/ml in methanol) for 20 min, then removed from the PVP solution and the solvent was allowed to evaporate at room

temperature. Finally the electrode was rinsed with pure water. For this electrode, the CoTsPc was expected to be between the OPG and PVP layer.

(2) **OPG/(CoTsPc + PVP)**

The OPG electrode was immersed in a solution containing 1 x 10^{-4} M CoTsPc and 8 x 10^{-4} mg/ml PVP in 1:9 water/methanol mixture (saturated with air) for 20 min with the electrode rotating at ~30 rpm. The electrode was then removed from the solution and washed with pure water. This electrode was expected to have CoTsPc in the PVP layer.

(3) **OPG/PVP/CoTsPc**

The OPG electrode was first coated with a thin film of PVP formed by applying ~6 μl of PVP solution (8 x 10^{-4} mg/ml in methanol) to the OPG surface and evaporating off the solvent at room temperature. After rinsing with pure water the electrode was then immersed in 1 x 10^{-4} M CoTsPc solution in water (air saturated) for 15 min with the electrode rotating at ~30 rpm. The electrode was again washed with water. In this case the CoTsPc was expected to be adsorbed on top of the PVP layer. The estimated thickness of the PVP layer was ~0.02 nm as determined from the concentration of the PVP solution in methanol, the volume of this solution applied to the electrode surface and the estimated density of the PVP.

Cyclic voltammetry

Cyclic voltammetry with OPG electrodes were obtained in N_2 or O_2 saturated 0.05 M H_2SO_4 solutions. Figure 12 shows the cyclic voltammograms on OPG and OPG/PVP electrodes in a N_2-saturated solution. The slight change in the voltammetry curve obtained by the PVP layer may have been produced by a slight increment in the effective electrode area resulting from the penetration of the PVP into the surface fissures in the OPG. An alternate explanation is that the intrinsic capacitance of the OPG - PVP interface is slightly larger than that

of the OPG-water interface. It indicates that the thin film of PVP on the OPG electrode surface does not cause any significant change in electrochemical behavior of the OPG electrode in acid solution. Peak c corresponds to the redox behavior of quinone/hydroquinone functional groups on the OPG surface (16). Figure 13 shows the cyclic voltammogrms on OPG/CoTsPc and OPG/PVP/CoTsPc electrodes in N_2 saturated 0.05 M H_2SO_4. According to Zecevic et al. (3), the peaks a', b' and d' can be assigned as follows:

Peak a': Co(I)TsPc(-2)/Co(I)TsPc(-3), H^+

Peak b': Co(II)TsPc(-2)/Co((I)TsPc(-2), H^+

Peak d': Co(III)TsPc(-2)/Co(II)TsPc(-2)

The peak c' in Fig. 13 corresponds to peak c in Fig. 12. The peaks e and e' with and without PVP as well as some additional small peaks with PVP in Fig. 13 are not clear at present. The potentials of peaks a, b and d with PVP are somewhat different from the peak potentials of a', b' and d' without PVP indicating some interaction of PVP with CoTsPc (as discussed later). Similar changes are observed with OPG/CoTsPc/PVP and OPG/CoTsPc+PVP modified electrodes.

Figures 14 and 15 show the cyclic voltammograms with OPG, OPG/PVP, OPG/CoTsPc and OPG/CoTsPc/PVP electrodes in O_2 saturated 0.05 M H_2SO_4. Figure 14 shows that the PVP film on the surface of OPG electrode does not cause a significant change in either the peak potential or the peak current for O_2 reduction, but does show some minor changes which suggest that the transport of O_2 to the OPG surface is somewhat inhibited. In acid solutions, PVP is an ionic conductor. The O_2 reduction in the absence of any other catalyst than the OPG itself must occur on the OPG surface. The catalytic action of the OPG, is very low in acid solution. Figure 15 shows that the peak potential for O_2 reduction on OPG/CoTsPc is more positive than that of OPG alone and further positive shift in the peak potential is obtained (about 0.14 V vs. SCE) when

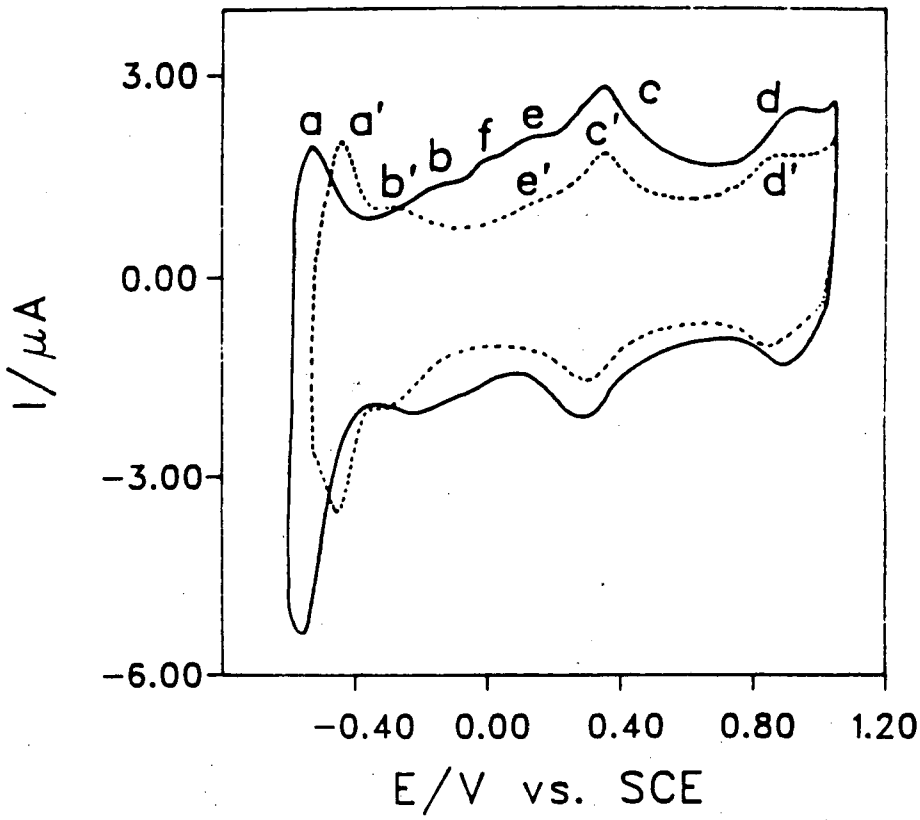

Fig. 13. Cyclic voltammograms on OPG/CoTsPc (----) and OPG/PVP/CoTsPc (——) electrodes in N_2-saturated 0.05 M H_2SO_4 solutions. Scan rate = 200 mV/s. Undashed symbols with PVP and dashed symbols without PVP.

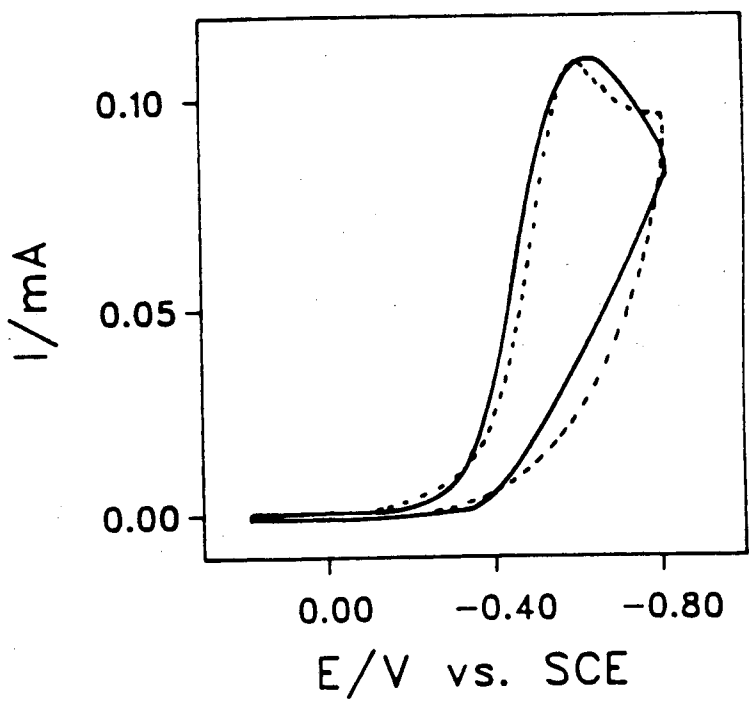

Fig. 14. Cyclic voltammograms on OPG (----) and OPG/PVP (——) electrodes in O_2-saturated 0.05 M H_2SO_4 solutions. Scan rate = 100 mV/s.

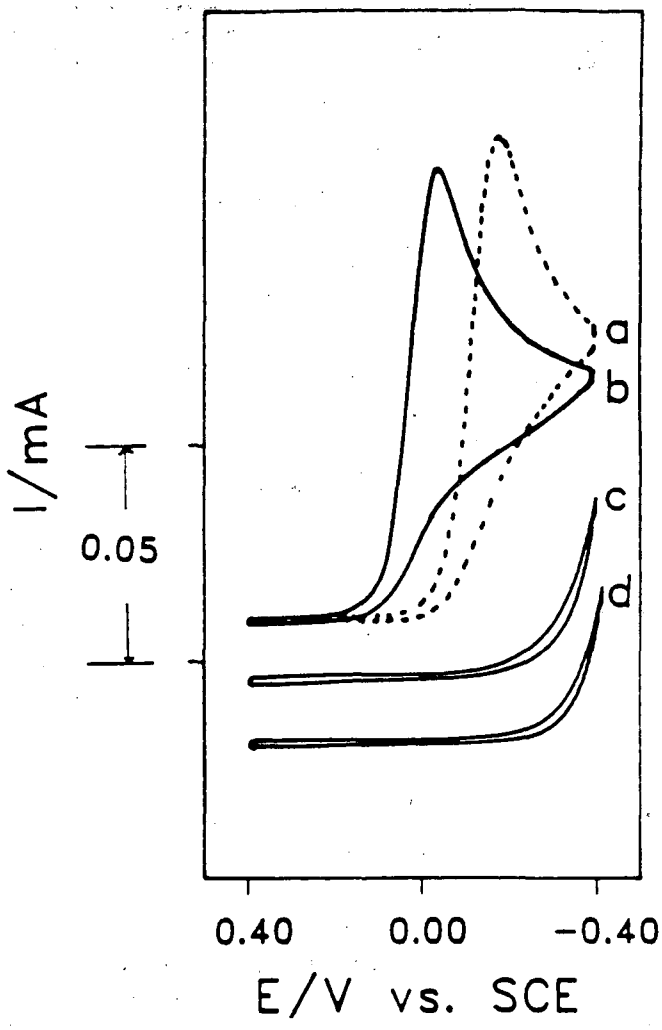

Fig. 15. Cyclic voltammograms on various electrodes in O_2-saturated 0.05 M H_2SO_4 solutions. (a) OPG/CoTsPc; (b) OPG/CoTsPc/PVP; (c) OPG/PVP and (d) OPG. Scan rate = 100 mV/s.

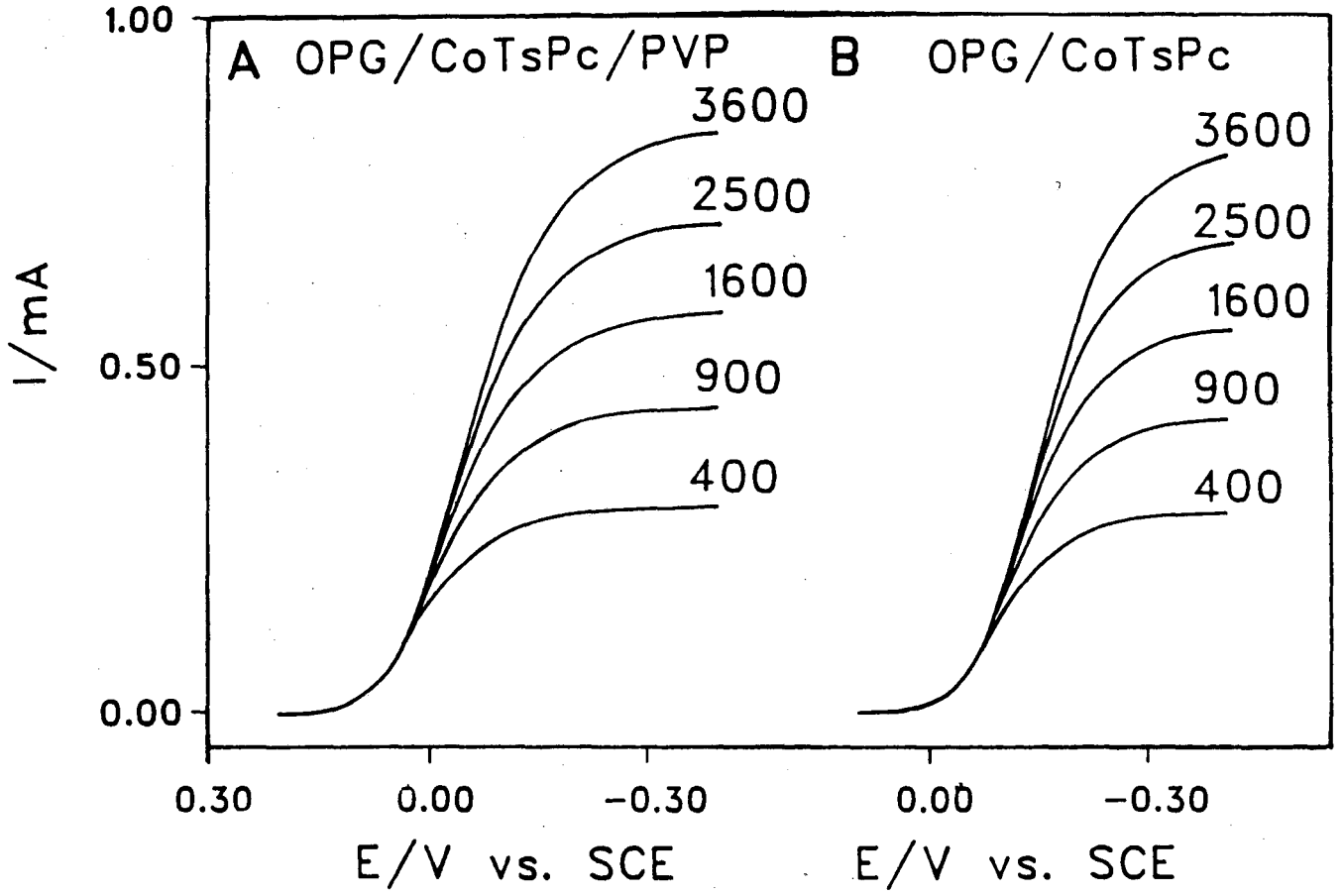

Fig. 16. Current-potential curves for O_2 reduction on rotating (A) OPG/CoTsPc/PVP and (B) OPG/CoTsPc disk electrodes in O_2-saturated 0.05 M H_2SO_4 solutions. Scan rate = 10 mV/s. The number above each curve indicates the corresponding rotation rate in rpm.

OPG/CoTsPc electrode is coated with a thin layer of PVP. It is thus clear that the OPG/CoTsPc/PVP electrode exibits higher catalytic activity for O_2 reduction than OPG/CoTsPc in acid electrolytes.

O_2 reduction

Figure 16 shows the current-potential curves for O_2 reduction at OPG/CoTsPc and OPG/CoTsPc/PVP electrodes at different rotation rates in O_2-saturated 0.05 M H_2SO_4 solutions. The half-wave potential ($E_{1/2}$) shifts by about 0.11 V more positive for the PVP-modified electrode than the corresponding unmodified electrode, but the limiting current is nearly the same, indicating negligible inhibition in the diffusion of O_2 through the PVP film of such thickness.

For a rotating disk electrode experiment involving a totally irreversible electrode process which is first order for reactant, the measured current i is given by (17)

$$1/i = 1/i_k + 1/i_d = 1/i_k + 1/B\omega^{1/2} \quad (1)$$

where i_k is the kinetic current, i.e., the current in the absence of mass transport control, i_d is the diffusion limiting current, ω is the rotation rate and B is a constant independent of rotation rate. An expression for i_d is given by

$$i_d = B\ \omega^{1/2} \quad (2)$$

$$B = 0.62nFAC_o^*D_o^{2/3}\nu^{-1/6} \quad (3)$$

where n is the overall number of electrons transferred per O_2 molecule, A is the electrode area, C_o^* is the bulk concentration of the reactant, D_o is the diffusion coefficient of the reactant and ν is the kinematic viscosity.

According to Eq. (1), a plot of i^{-1} vs $\omega^{-1/2}$ should be linear with an intercept equal to i_k^{-1} and slope equal to 1/B. i_k and B can thus be obtained.

Figure 17 shows the plots of i^{-1} vs $\omega^{-1/2}$ from the data (without PVP) in

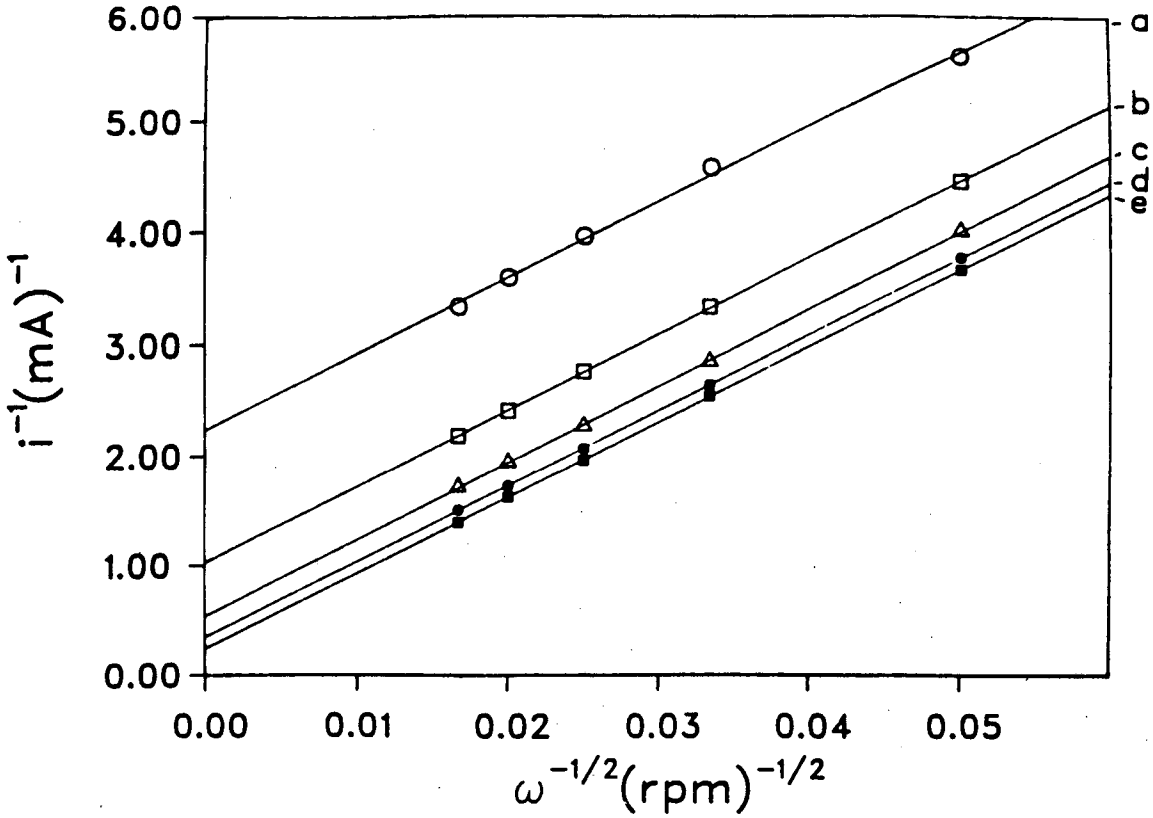

Fig. 17. Koutecky-Levichs plots for O_2 reduction on OPG/CoTsPc electrode at potentials of a, -0.2; b, -0.23; c, -0.26; d, -0.29 and e, -0.32 V. Data from Fig. 5(B).

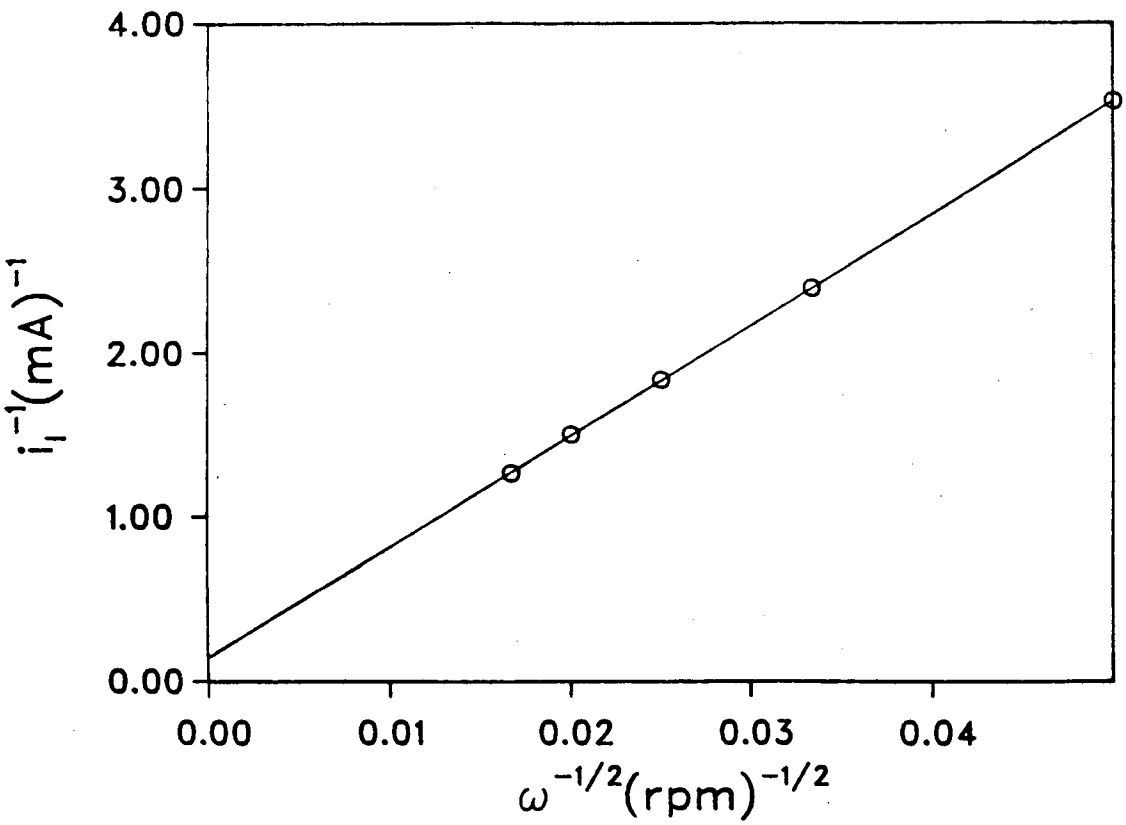

Fig. 18. Plot of i_{lim}^{-1} vs $\omega^{-1/2}$ for O_2 reduction on OPG/CoTsPc/PVP electrode in O_2-saturated 0.05 M H_2SO_4 solutions. Scan rate = 10 mV/s.

Table IV Kinetic currents at different potentials for O_2 reduction on various electrodes in 0.05 M H_2SO_4

E/V vs.SCE	i_k(mA cm^{-2}) OPG/PVP/CoTsPc	OPG/(PVP+CoTsPc)	OPG/CoTsPc/PVP	OPG/CoTsPc	E_F*
-0.14	10.63	12.07	17.04	2.28	7.47
-0.18	19.85	20.76	33.11	4.95	6.69
-0.22	34.15	38.16	58.92	9.43	6.25
-0.26	72.58	72.78	82.83	14.49	5.71

*E_F(Enhancement Factor)=[i_k on (OPG/CoTsPc/PVP)/i_k on (OPG/CoTsPc)]

Table V Assignment of some spectral features of DRIFT spectra of PVP, adduct I and adduct II (in KBr)

Ligand and adducts	Assignment, cm^{-1} $\nu_{C=C,C=N}$	$\nu_{C=C}$	δ_{CH}(in plane)	δ_{CH}(out of plane)
PVP	1597	1495	995	824
Adduct I	1637, 1601	1506	1007	827
Adduct II	1637, 1605	1504	1010	826

Table VI Voltammetric peak potentials(vs. SCE) for O_2 reduction in various electrolyte solutions

Electrolyte	E_{pc}/V OPG/CoTsPc	E_{pc}/V OPG/CoTsPc/PVP	E_{pc}/V OPG/PVP/CoTsPc
0.05 M H_2SO_4	-0.19	-0.05	-0.07
Phosphate buffer (pH = 7.4)	-0.40	-0.45	-0.57
0.1 M NaOH	-0.40	-0.44	-0.52

Table VII The effect of thickness(t)[1] of PVP film on OPG electrode with adsorbed CoTsPc on catalytic activity for O_2 reduction in 0.05 M H_2SO_4 solution (rotation rate, 2500 rpm; scan rate, 10 mV/s)

t(μm)	0	0.002	0.01	0.02	0.1	0.2
C*(mol cm^{-2})	0	1.7×10^{-9}	8.5×10^{-9}	1.7×10^{-8}	8.5×10^{-8}	1.7×10^{-7}
$E_{1/2}$(V)	-0.175	-0.078	-0.076	-0.067	-0.075	-0.088
i_d(mA)	0.645	0.645	0.640	0.640	0.620	0.620

* C = concentration of PVP unit on the OPG surface

1. The thickness of PVP film was estimated approximately from the bulk density of PVP (0.85 g/ml), concentration of the PVP solution in the methanol and the volume of this solution applied to the surface.

Fig. 16(B) for O_2 reduction on the OPG/CoTsPc electrode. The i_k values calculated from the intercepts are shown in Table IV.

For a polymer-modified electrode, as for example, OPG/CoTsPc/PVP electrode, the limiting current (i_{lim}) for O_2 reduction is given by (18,19)

$$1/i_{lim} = 1/i_f + 1/i_d = 1/i_f + 1/B\omega^{1/2} \quad (4)$$

where i_f is the current controlled by O_2 diffusion through the polymer film. Plot of i_{lim}^{-1} vs $\omega^{-1/2}$ should be linear and i_f^{-1} can be obtained from the intercept.

The measured current (i) for the PVP-modified electrode at any point on the current-voltage curve is given by

$$1/i = 1/i_k + 1/i_f + 1/B\omega^{1/2} \quad (5)$$

According to Eq. (5), a plot of i^{-1} vs $\omega^{-1/2}$ should be linear and $(1/i_k + 1/i_f)$ can be obtained from the intercept. Since i_f^{-1} can be obtained from the plot of i_{lim}^{-1} vs $\omega^{-1/2}$, then i_k can be calculated for the modified electrode.

Figures 18 and 19 show the plots of i_{lim}^{-1} vs $\omega^{-1/2}$ and i^{-1} vs $\omega^{-1/2}$, respectively. The i_k obtained from the data in Fig. 16(A) for O_2 reduction on the OPG/CoTsPc/PVP electrode are listed in Table IV.

The data from Table IV show that the kinetic current is much higher on the OPG/CoTsPc/PVP electrode than on the OPG/CoTsPc electrode at the same potential. The enhancement factors (20) (see Table IV) are quite large.

From Figs. 17 and 19, we find that the plots of i^{-1} vs $\omega^{-1/2}$ at various potentials are linear and parallel to one another. This confirms that the rate of O_2 reduction on OPG/CoTsPc/PVP electrodes is first order with respect to O_2 as is case for OPG/CoTsPc electrodes. The B values determined from Figs. 17 and 19 are equal to 1.46×10^{-2} mA(rpm)$^{-1/2}$ and 1.47×10^{-2} mA(rpm)$^{-1/2}$, respectively. These values agree well with the calculated value (1.42×10^{-2} mA(rpm)$^{-1/2}$) (16) from Eq. (3) for n = 2, indicating that O_2 reduction proceeds through a 2-electron pathway leading to H_2O_2 on these electrodes.

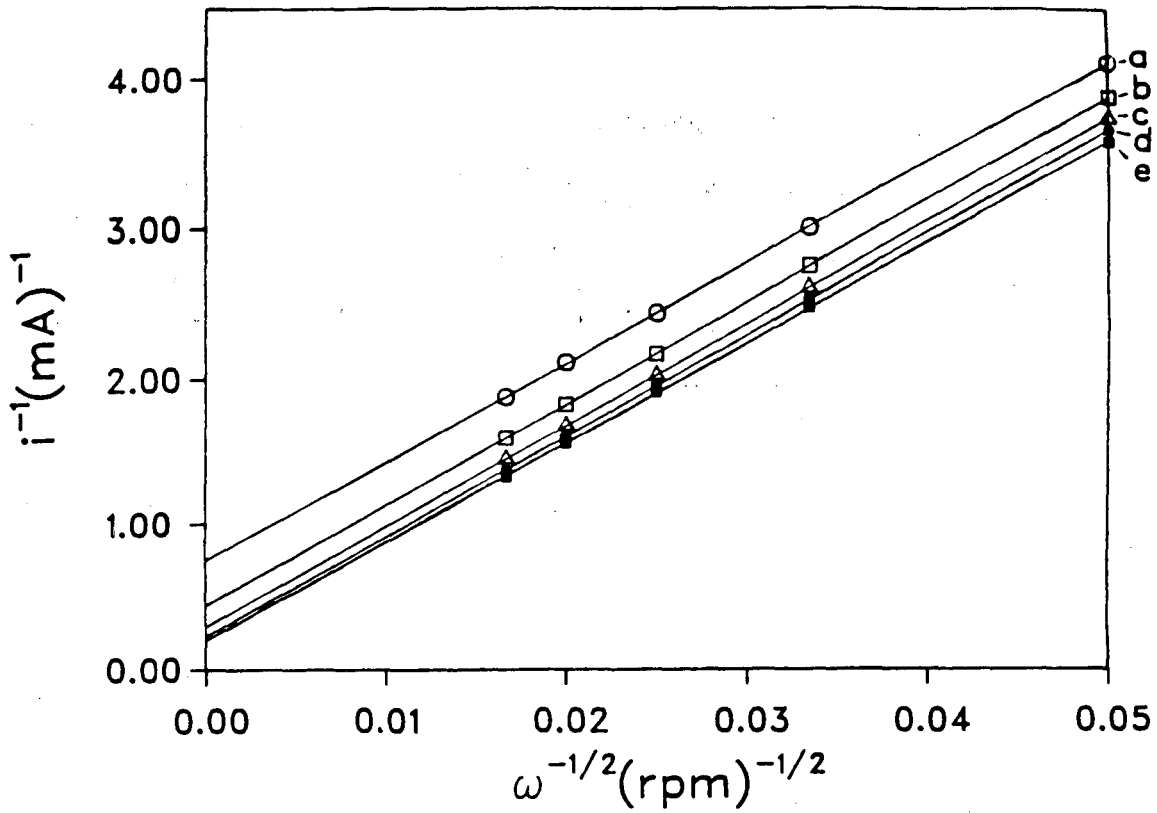

Fig. 19. Koutecky-Levich plots for O_2 reduction on OPG/CoTsPc/PVP electrode at potentials of a, -0.03; b, -0.07; c, -0.11; d, -0.15 and e, -0.19 V. Data from Fig. 5(A).

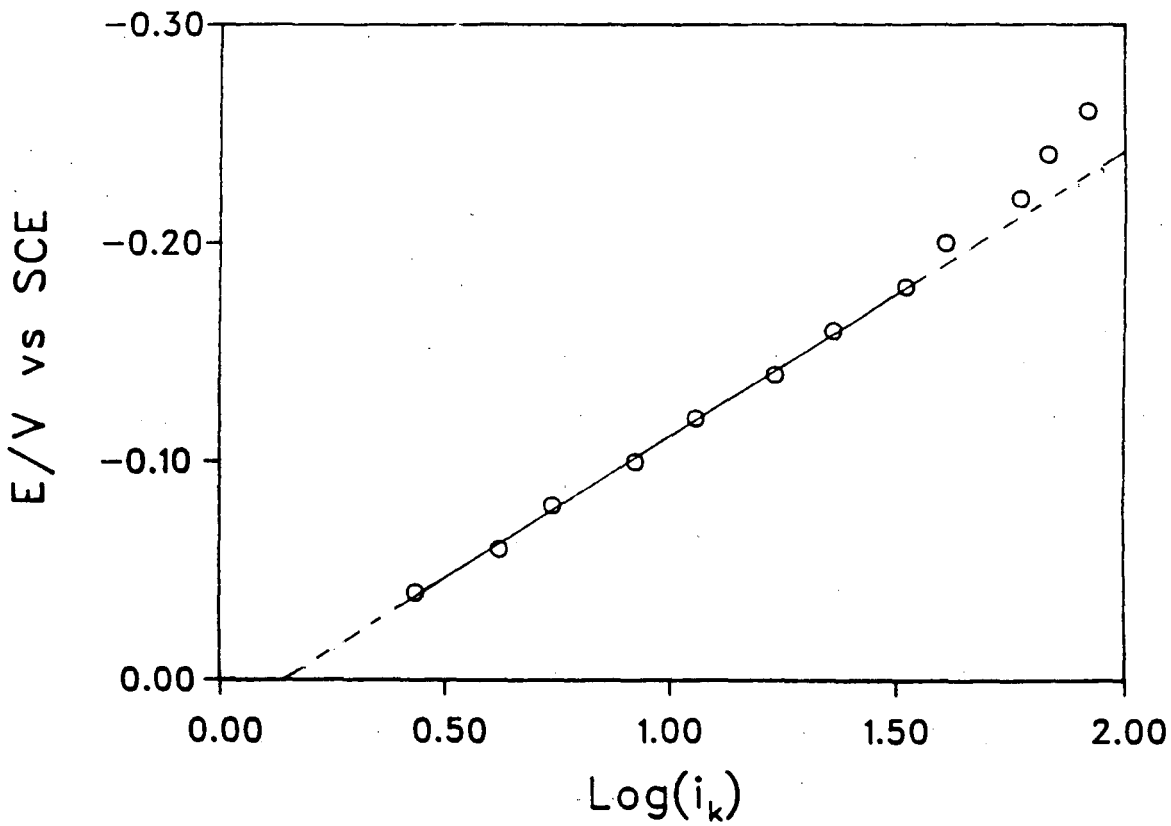

Fig. 20. Tafel plot for O_2 reduction on OPG/CoTsPc/PVP electrode in O_2-saturated 0.05 M H_2SO_4 solutions. Data from the intercepts in Fig.8.

Figure 20 shows the disk potential E vs $\log(i_k)$ plot (Tafel plot) for the modified electrode. It exhibits linear behavior over two decades with a slope of -130 mV/decade at ~22°C. The upper section of the plot at potential numerically greater than -0.20 V is limited by the accuracy with which the intercepts in Fig. 19 could be determined. This value is close to the theoretically expected value of -118 mV/decade for an apparent transfer coefficient $\alpha = 0.5$ with a first one-electron-transfer rate controlling step at ~22°C, i.e.,

$$O_2(ads) + e^- \rightarrow O_2^-(ads)$$

This supports the mechanism for O_2 reduction on graphite proposed by Morcos and Yeager (21).

The effect of the polymer film on the kinetics of O_2 reduction

Figure 21 shows the comparison of polarization curves for O_2 reduction at a rotation of 2500 rpm for various PVP-modified electrodes in 0.05 M H_2SO_4 solution saturated with O_2. The curves a, b, and c with polymer films are close to each other and the rising portions of O_2 reduction waves shift positive relative to the curve d without the film. The kinetic currents i_k for O_2 reduction on OPG/CoTsPc/PVP, OPG/(CoTsPc+PVP) and OPG/PVP/CoTsPc electrodes are also listed in Table IV, which are close to each other. In order to explain these results and the fact that the OPG/CoTsPc electrode modified by PVP exhibits higher electrocatalytic activity for O_2 reduction in acid medium, the interaction between CoTsPc and PVP must be considered.

Interactions between PVP and CoTsPc

In O_2 reduction electrocatalysis involving transition metal macrocycles, the nature of the cheleting agent and the central ion play an important role [22]. In the polymer-modified electrode, the interactions between the transition metal macrocycle and the polymer must be considered. These interactions

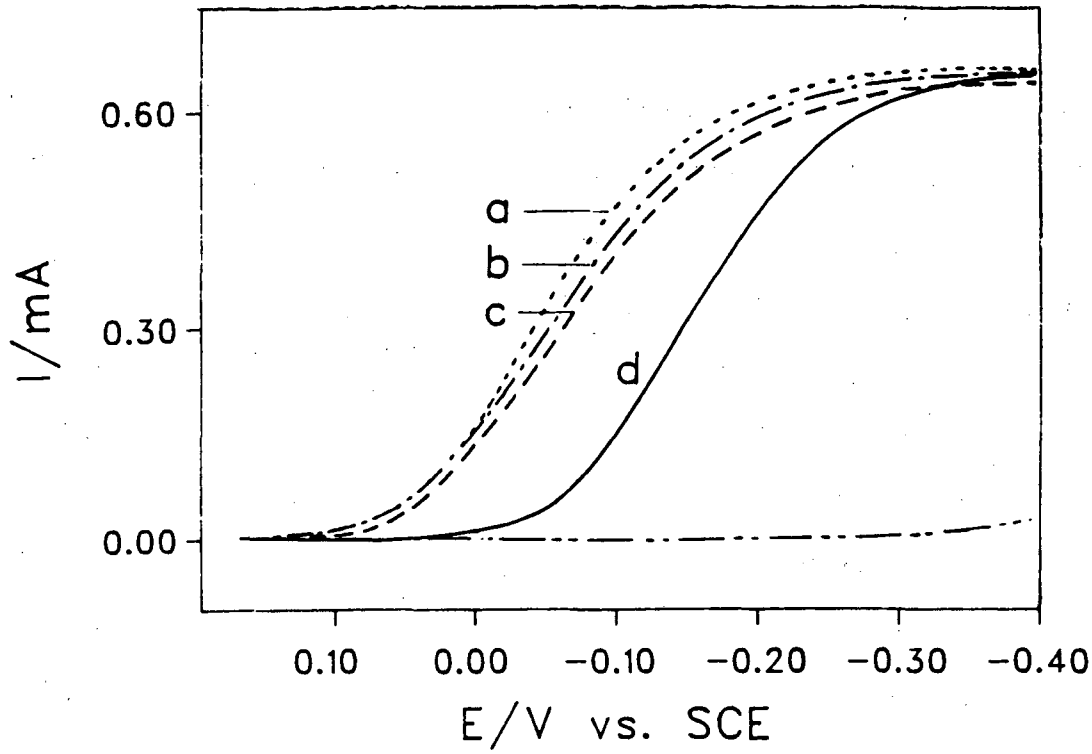

Fig. 21. Rotating-disk voltammograms for O_2 reduction in O_2-saturated 0.05 M H_2SO_4 solutions. (a) OPG/CoTsPc/PVP (····); (b) OPG/(PVP+CoTsPc) (–·–·); (c) OPG/PVP/CoTsPc (----); (d) OPG/CoTsPc (——) and (e) OPG (–··–··). Rotation rate = 2500 rpm; scan rate = 10 mV/s.

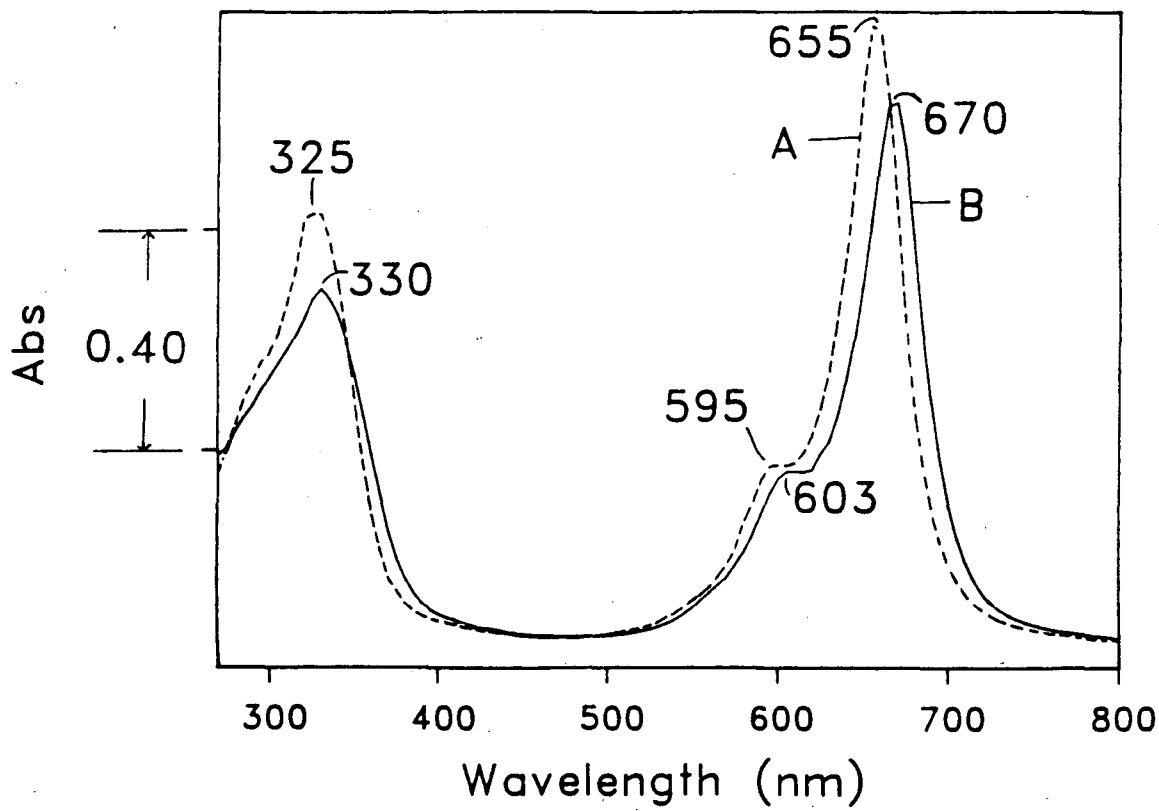

Fig. 22. Uv - visible absorption spectra for (A) $1x10^{-4}$ M CoTsPc and (B) $1x10^{-4}$ M CoTsPc + $8x10^{-4}$ mg/ml PVP in 1:9 water/methanol mixture. Cell length = 1.00 cm. The number near a peak indicates the corresponding peak position in nm.

may include the chemical bonding and electrostatic interactions. With OPG-CoTsPc-PVP, both chemical and electrostatic interactions must be considered. Some information concerning these interactions can be obtained from spectroscopic studies of the layers and the solution phase. Figure 22 shows the uv-visible absorption spectra obtained with solutions one of which is 1×10^{-4} M CoTsPc and the second is 1×10^{-4} M CoTsPc + 8×10^{-4} mg/ml PVP, both solutions using a 1:9 water/methanol solvent. The 325, 595 and 655 nm absorption bands for the CoTsPc solution without PVP shift to 330, 603 and 670 nm, respectively, for the same solution with PVP.

Figure 23 gives the infrared spectra of PVP, CoTsPc and the adducts formed between CoTsPc and PVP in a KBr matrix using diffuse-reflectance infrared Fourier transform spectroscopy. It is seen from Table V that the absorption of PVP at 1597 cm^{-1} for $\nu_{C=C,C=N}$ of the PVP pyridine ring shifts to 1637 cm^{-1} in both adduct I and adduct II. This supports the coordination between pyridine of the PVP and the cobalt of CoTsPc. The band around 1601 cm^{-1} in adduct I and around 1605 cm^{-1} in adduct II may correspond to the uncoordinated pyridine of the PVP in the adducts. The absorption peaks due to the $\nu_{C=C}$, δ_{CH}(in plane) and δ_{CH}(out of plane) of PVP also shift to a higher wavenumber by 9 - 11, 12 - 15 and 2 - 3 cm^{-1} respectively in the adducts. The results summarized in Table V are very similar to the results obtained by Kurimura et al. (23) for the complexes of PVP with cis-$[Co(en)_2Cl_2]Cl$ and cis-$[Co(trien)Cl]Cl_2$ and suggest the coordination of cobalt in CoTsPc with pyridinium-nitrogen of PVP through the axial position of the transition metal.

Although the peak shifts for both adduct I and adduct II are similar as seen from Table V, there are certain differences in the infrared spectra for the two adducts. The absorption peaks around 1194 and 1032 cm^{-1} involving the asymmetric and symmetric stretching vibrations of $-SO_3^-$ in CoTsPc shift to lower wave numbers, 1175 and 1024 cm^{-1}, respectively, in adduct II. The shift

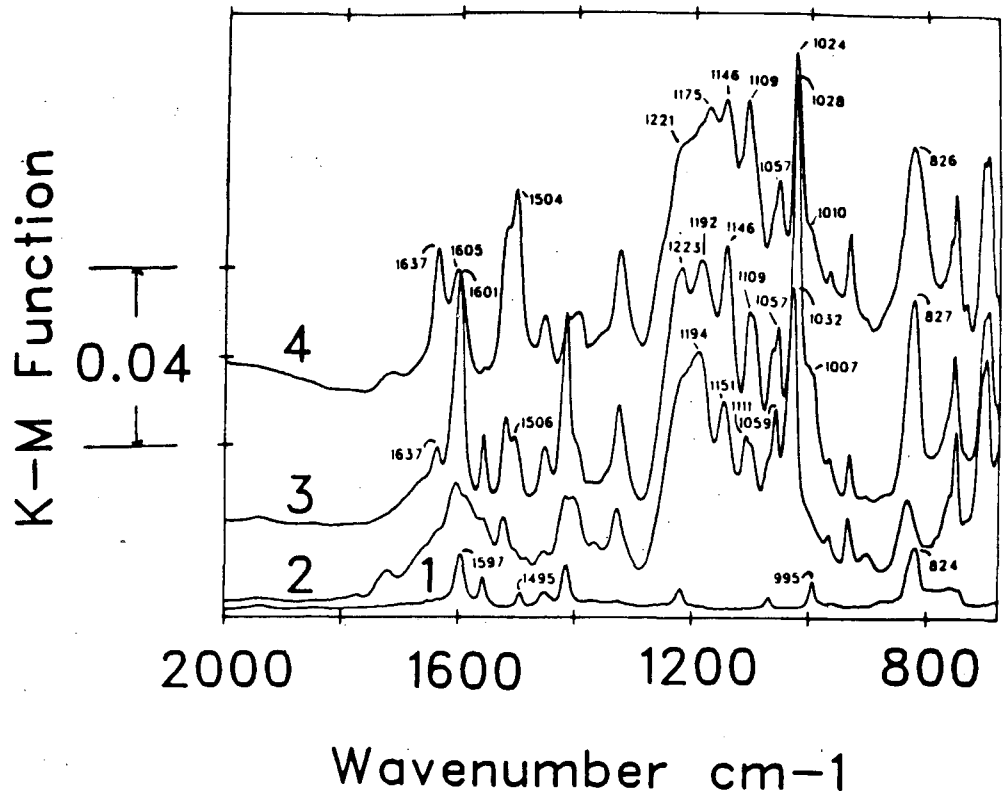

Fig. 23. Diffuse reflectance FTIR spectra of 1, PVP, 0.1 wt%; 2, CoTsPc, 0.5 wt%; 3, adduct I, 0.6wt% and 4, adduct II, 0.6 wt% in KBr. Grinding time = 5 min. The K-M function = $(1 - R)^2/2R$, where R is the reflectance (see Ref. 11). The small number in the figure indicates the correponding peak position in cm^{-1}.

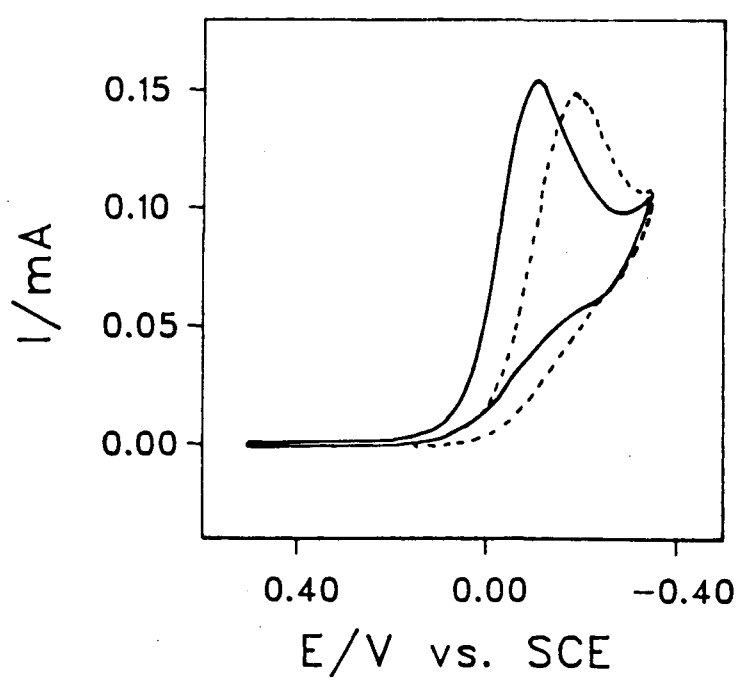

Fig. 24. Cyclic voltammograms on OPG/CoPc/PVP (——) and OPG/CoPc (----) electrodes in O_2-saturated 0.05 M H_2SO_4 solutions. Scan rate = 10 mV/s.

of these peaks results from some kind of interaction of the PVP polymer with the $-SO_3^-$ group in CoTsPc. It may be explained that besides the coordination of pyridinium-nitrogen of PVP with cobalt in CoTsPc, there is an electrostatic interaction as well between $-SO_3^-$ group and protonated pyridinium units which are uncoordinated in the PVP. If 0.05 M H_2SO_4 is added to the solution containing 8 x 10^{-4} mg/ml PVP and 1 x 10^{-4} M CoTsPc in 1:9 water/methanol mixture, a dark blue precipitate appears immediately corresponding to the formaton of adduct II.

When either of the adducts is adsorbed on the OPG electrode from its solution in DMSO, it shows much better catalytic activity for O_2 reduction in 0.05 M H_2SO_4 solutions than the OPG electrode with only adsorbed CoTsPc and closely similar activity to the PVP-modified OPG electrode with adsorbed CoTsPc.

Cobalt phthalocyanine which has no $-SO_3^-$ group was used to replace CoTsPc for comparison. The preparation of the modified electrode for CoPc is same as CoTsPc except the CoPc was adsorbed from a DMSO solution. Figure 24 shows the cyclic voltammograms with OPG/CoPc/PVP and OPG/CoPc electrodes in O_2-saturated 0.05 M H_2SO_4 solution. The catalytic activity for O_2 reduction is higher on OPG/CoPc/PVP electrode than on OPG/CoPc electrode. This also can be explained by the formation of an adduct between CoPc and PVP on the OPG electrode surface. The only strong interaction between the CoPc and PVP in this adduct is the coordination of the pyridine in PVP with the Co in CoPc.

Influence of pH on catalytic activity for O_2 reduction

Table VI shows the peak potentials for O_2 reduction, which are obtained from cyclic voltammograms on OPG/CoTsPc, OPG/CoTsPc/PVP and OPG/PVP/CoTsPc electrodes in 0.05 M H_2SO_4, phosphate buffer and 0.1 M NaOH solutions saturated with O_2. For a totally irreversible system the peak potentials are expected to

be a linear function of $\ln(k^o)$, where k^o is the first-order standard rate constant (17). The OPG/CoTsPc/PVP electrodes exhibit higher catalytic acivity for O_2 reduction, as compared with OPG/CoTsPc electrodes in acid solutions. In the neutral and alkaline solution, however, a similar OPG/CoTsPc/PVP electrode inhibits O_2 reduction as compared to the OPG/CoTsPc electrode without PVP. These inhibition effects may be due to the formation of a unprotonated poorly conducting PVP film in the case of the OPG/CoTsPc/PVP on the electrode surface which reduces the diffusion of O_2 through the film and increases the ohmic resistance. Similar inhibition was obtained with an OPG electrode coated with PVP layer without the macrocycle.

Influence of the thickness of PVP films

In order to investigate the effect of the thickness of PVP film on the electrode surface on catalytic activity for O_2 reduction, the thickness of the PVP film coated on the electrode surface was varied by changing the concentration of the PVP solution keeping the solution volume constant. The results are given in Table VII. In the thickness range of the PVP film between 0.002 and 0.1 μm, the differences in $E_{1/2}$ are practically negligible. However, when the thickness of the PVP film increases further, the $E_{1/2}$ shifts negatively and the i_d decreases as shown in Table VII for OPG/PVP/CoTsPc electrode.

Catalytic stability of the CoTsPc-PVP-modified electrode

The OPG/CoTsPc/PVP and OPG/CoTsPc electrodes were used for comparison of the catalytic stability for O_2 reduction in O_2-saturated 0.05 M H_2SO_4 solutions. O_2 was blown through the solution continuously and the electrode was rotated at 2500 rpm while maintaining the electrode potential at $E_{1/2}$. Over a ten-hour period, the activity of the OPG/CoTsPc/PVP system was essentially constant while that of OPG/CoTsPc (no polymer) decreased by a substantial amount (~37%) indicating that the PVP layer prevents the diffusion of the CoTsPc complex as a whole and/or the cobalt from the complex into the solution.

The other interpretation of this effect may be due to the fact that the adduct formed between PVP and CoTsPc is insoluble in a 0.05 M H_2SO_4 solution.

F. Transition metal oxide catalysts: pyrochlores and lithiated NiO

F-1. Pyrochlores

Metallic oxides with the pyrochlore structure have attracted attention in recent years for their catalytic activity both for O_2 reduction and generation. The pyrochlores were used at CWRU together with carbon black or heat-treated macrocycle/carbon in order to optimize the O_2 reduction performance. Recently lead ruthenate pyrochlore $Pb_2Ru_2O_{6.5}$ was used successfully in a self-supporting mode, without high-area carbon as catalyst support. Carbon is oxidized in both acid and alkaline electrolytes at even moderate temperatures (i.e., 200°C) and this sets a limit on the useful life of high performance air electrodes.

Anion-exchange membranes (RAI-4085) applied to the solution side of the porous gas-fed electrodes were found at CWRU to improve greatly the performance of pyrochlore-based bifunctional oxygen electrodes when operating in the O_2 generation mode. This was believed to result partly from the membrane's ability to retard the transport of soluble Pb and Ru species out of the porous electrode. During the past year, spectrophotometric techniques were used to measure the concentration of the orange ruthenate anion, $HRuO_4^-$ which builds up in the electrolyte during anodic polarization without the membrane present. The ruthenate concentration was determined from the absorbance of the 5.5 M KOH solution at 465 nm. In these preliminary experiments the anodic polarization was determined at several different current densities, from 1 mA/cm^2 to 13 mA/cm^2. Further work is in progress using potentials. In the preliminary experiments it was found that the membrane prevented the build-up of measurable amounts of ruthenate in the electrolyte at a curent density of 2 mA/cm^2 (potential of approximately 0.437 V vs. Hg/HgO, OH^-) for one hour. A similar

electrode without a membrane lost ~12% of its ruthenium content under similar conditions. Further experiments are planned at high current densities and more anodic potentials. In earlier work at CWRU with Pb ruthenates as anode catalyst, the lead was introduced into the electrolyte and then deposited with cathode, often in dendritic form. Such effects can be suppressed with proper use of ionic conducting membranes.

The pyrochlore used in these measurements was high area $Pb_2Ru_2O_{6.5}$ prepared at ~90-100°C but not heat treated further. The heat-treated pyrochlore (~300°C) was much more corrosion-resistant. At higher current densities the experiment is complicated by the cathodic deposition of hydrate RuO_2 at the counter electrode, which removes Ru(VI) from the solution. In further experiments, the counter electrode will be shielded using an anion exchange membrane.

In overall prospective, the use of a membrane offers opportunities for major advances in gas-fed air electrodes in which the fluid electrolyte within the electrode is replaced with an ionic conducting polymer. The long-term stability of the electrode can be significantly improved and the polarization reduced. In some instances, just applying a thin ionic conducting polymer layer on the solution side is sufficient to stabilize the electrode by retarding transport of catalyst compounds out of the membrane.

F-2. Lithiated NiO

The temperature dependence of the kinetics of the O_2 reduction and generation reactions has not been systematically examined on oxide catalysts in alkaline solutions over a wide temperature range (≤250°C). Some oxides such as p-type nickel oxide are very ineffective as O_2 reduction catalysts at low and moderate temperatures but become quite active at higher temperatures, particularly above the Neel temperature. Just what factors are involved warrant investigation for both fundamental and experimental reasons.

NiO(Li) is being examined as a catalyst for O_2 reduction and generation at

elevated temperatures, i.e., 200°C, in concentrated KOH. At these temperatures, the O_2 kinetics become essentially reversible at low currents and show surprisingly low polarization. The research is designed to establish what changes in the electronic, magnetic and lattice properties of the NiO(Li)-KOH systems are responsible for the large increase in catalytic activity at temperatures approaching 200°C. At lower temperatures, (<150°C), NiO(Li) is a poor catalytic surface for reduction processes such as O_2 reduction which require n-type rather than p-type semiconductors.

Experiments have been carried out thus far using PTFE-bonded porous electrodes in the floating electrode mode, principally with $Ni_{0.9}Li_{0.1}O$. The temperature dependence of the magnetic susceptibility is also being examined in order to test the hypothesis of Tseung that the catalytic activity for O_2 greatly increases when the temperature exceeds the Neel temperature, i.e., the material becomes paramagnetic. It should be noted, however, that the Neel temperature is a bulk magnetic property and that the effective temperature for the surface species of NiO lattice need not be the same as for the bulk oxide.

G. Electrocatalysts for bifunctional electrodes

G-1. Pyrochlores (use of pore-former)

The pyrochlore structure has been found to have high catalytic activity both for O_2 reduction and generation. The measurements with the pyrochlore $Pb_2Ru_2O_{6.5}$ in self-supported form (i.e., without high-area carbon in the active layer) have shown that the electrode structure and performance can be improved greatly with the use of pore-former such as ammonium bicarbonate. The O_2 reduction performance with such electrodes is now significantly better than previously achieved with carbon supports.

The fabrication method requires modification for the self-supported pyrochlore electrodes. For example, it was found necessary to employ a pore-

former material, ammonium bicarbonate, which is blended into the Teflon-pyrochlore mixture in powder form and is subsequently volatilized during the heat treatment of the electrode at ~300°C. It was found that excellent performance for O_2 reduction (Figs. 25, 26) is achieved when the resulting pores are of the order of 1 μm in diameter as was found in the SEM examination. These performance curves are among the best obtained at CWRU for any catalyst. The exact procedure for the incorporation of the pore-former was found to be of critical importance. A less favorable procedure led to much larger pores, in 10-20 μm range and the performance of such electrodes was quite poor and only slightly better than that for electrode fabricated without a pore-former.

In the anodic mode, loss of the pyrochlore into the bulk electrolyte is a problem. The application of an ionomer polymer to the solution side of the electrode does improve stability and activity in the anodic mode in KOH.

G-2. Preparation of pyrochlores with other platinum group metals substituted for ruthenium

Several samples of lead ruthenates were prepared with various amounts of platinum substituted for the ruthenium. It was found that the Horowitz alkaline-solution method could be adapted easily for these preparations. In preliminary testing of performance as catalysts for O_2 reduction with gas-fed electrodes using the $Pb_2Ru_{1.905}Pt_{0.095}O_{7-y}$ pyrochlore, however, no significant gain was found over the performance with the $Pb_2Ru_2O_{7-y}$ pyrochlore. The Pt material was amorphous. Further testing will employ more recent preparations, which are crystalline. Some samples of $Pb_2Ir_2O_{7-y}$ have also been prepared and will be tested shortly. The synthesis of $Pb_2Rh_2O_{7-y}$ will be attempted using the alkaline-solution method.

G-3. Iron-ruthenium perovskite as catalysts for bifunctional electrodes

In order to gain further understanding of the nature of ruthenium in various compounds as an electrocatalyst for O_2 reduction and generation, a

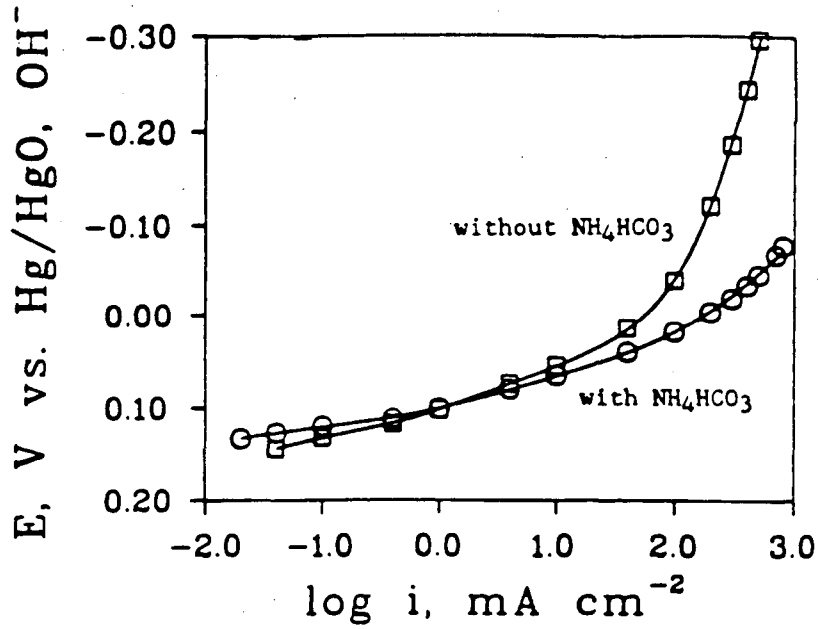

Fig. 25. Polarization curves for O_2 reduction with porous O_2-fed (1 atm) electrodes in 5.5 M KOH at -25°C. The electrodes contained 83.3 mg cm^{-2} pyrochlore and 27.8 mg cm^{-2} Teflon T30B and were heat-treated at 330°C for 2 h in flowing He. Ammonium bicarbonate (18.8 mg cm^{-2}) was added to one electrode as a pore-former before the heat treatment.

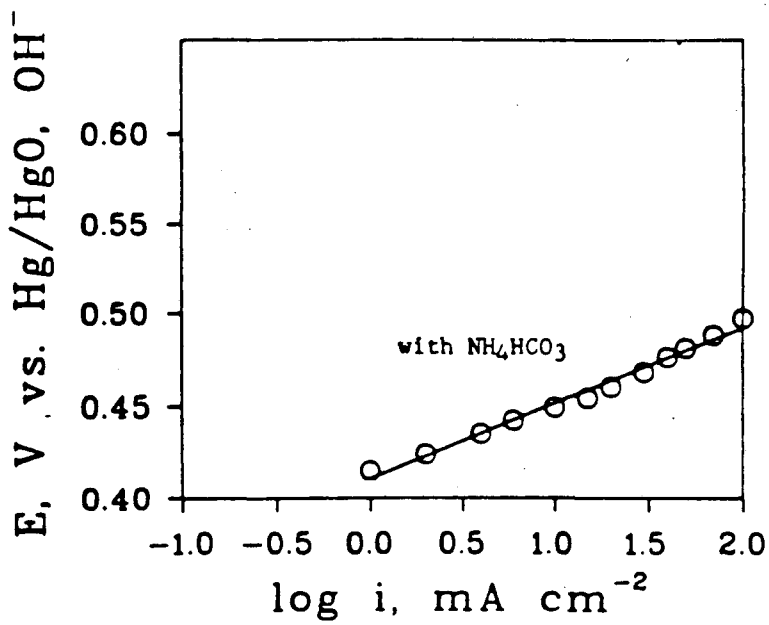

Fig. 26. Polarization curves for O_2 generation with a porous O_2-fed (1 atm) electrode in 5.5 M KOH at -25°C. The electrode contained 83.3 mg cm^{-2} pyrochlore and 41.7 mg cm^{-2} Teflon T30B and was heat-treated at 330°C for 2 h in flowing He. Ammonium bicarbonate (16.7 mg cm^{-2}) was added to the electrode as a pore-former before the heat treatment.

series of iron-ruthenium perovskite oxides was prepared and subjected to polarization measurements using gas-fed electrodes. This series of compounds can be described by the generic formula $SrFe_xRu_{1-x}O_{3-y}$. In terms of physical properties, this series exhibits variations in the electronic conductivity and magnetic behavior. For example, $SrRuO_3$ is at least one order of magnitude higher in conductivity although both are metallic conductors. Both are paramagetic at room temperature and above.

The O_2 reduction performance of the gas-fed electrodes improved steadily as x decreased i.e., as the ratio of Ru/Fe increased in alkaline solution (Figs. 27, 28). The mechanistic interpretation of the polarization curves is not straight forward because the electrode contained acetylene black to facilitate the fabrication process. In this case O_2 is probably reduced to peroxide on the carbon black, and the perovskite acts as a peroxide decomposer. The O_2 generation performance also improved steadily with increasing Ru content.

Other measurements, including Mossbauer spectroscopy and BET surface area, will be completed and will help to shed light on the physical basis of the electrocatalysis. Of particular interest are the coverage of different oxidation states of Fe and Ru and the presence of oxygen vacancies.

H. Catalyst supports

Most of the high-area carbons which are used as support materials for catalysts are generally considered to be unstable, particularly for O_2 generation. Efforts were made to find improved carbon supports. Several different carbon supports, including both fluorinated and non-fluorinated Shawinigan black and air oxidized and non-oxidized LBL graphitized carbon were examined at CWRU for use with lead ruthenate pyrochlore $Pb_2Ru_2O_{6.5}$.

During the past year use of mildly fluorinated carbon blacks as catalyst supports for platinum was explored in cooperation with the Electrosynthesis

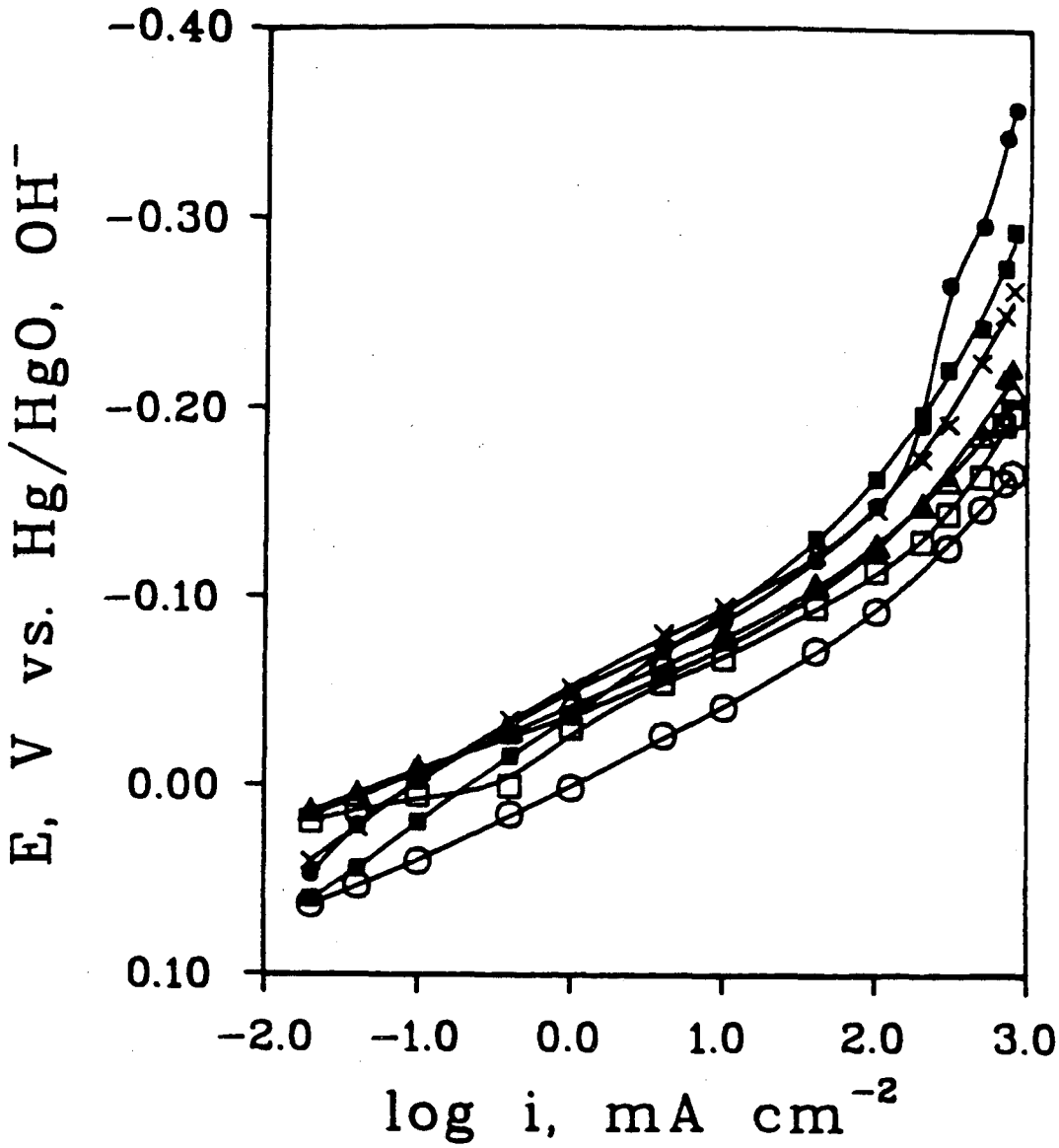

Fig. 27. Polarization curves for O_2 reduction on ruthenium perovskits ($SrFe_xRu_{1-x}O_3$) with a gas-fed (1 atm) electrode in 5.5 M KOH at 22°C. The electrode contained 15.8 mg cm^{-2} perovskite, 14.6 mg cm^{-2} air-oxidized Shawinigan acetylene black and 12.2 mg cm^{-2} Teflon T30B and was heat-treated at 280°C for 2 h in flowing helium. The curves are represented by the following values of x:

○: 0.0; □: 0.2; △: 0.4; ■: 0.5;

▲: 0.6; x 0.8; ●: 1.0

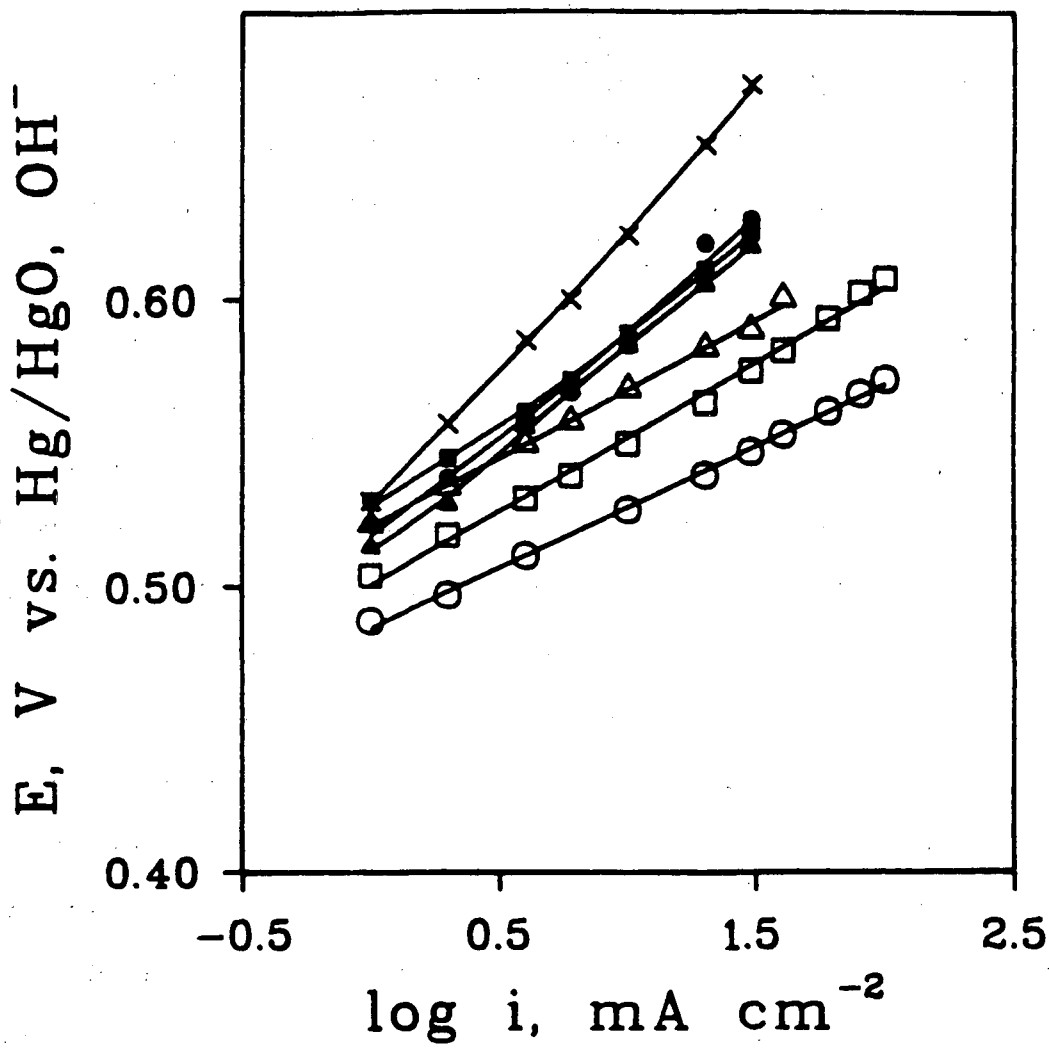

Fig. 28. Polarization curves for O_2 generation on ruthenium perovskites with a gas-fed electrode, Other conditions are the same as in Fig. V-13.
The curves are represented by the following values of x:

○: 0.0; □: 0.2; △: 0.4; ■: 0.5;

▲: 0.6; x 0.8; ●: 1.0

Company (ESC). ESC has developed the process of mild fluorination which converts certain types of oxygen-containing functional groups and edge-plane C-H groups without compromising the electronic conductivity.

Platinum was deposited on the fluorinated and non-fluorinated carbons and the catalyst then examined at CWRU using transmission electron microscopy (TEM) and gas-fed electrode measurements in 85% H_3PO_4 at 100°C. The Pt dispersions on the fluorinated carbons, in most cases, showed some non-uniformity and slightly larger particle sizes in comparison to that obtained for the non-fluorinated carbons. The O_2 reduction performance was slightly poorer in most cases for the gas-fed electrode made from the fluorinated carbons. The slightly higher polarization with the fluorinated carbon probably reflects the fact that the formulations and preparation of the porous gas-fed test electrodes were not yet optimized for this type of catalyst/support systems. Such optimization is very time consuming because a number of parameters are involved. This work was partially supported by a phase I DOE-SBIR contract through Electrosynthesis Company, NY. Efforts to improve the Pt dispersion and O_2 reduction performance will be undertaken in further work supported through a phase II DOE contract. Fluorination of heat-treated transition metal macrocycle/carbon catalysts will also be undertaken as part of the LBL-sponsored research.

V. FUTURE WORK

1. Structural studies of adsorbed macrocycle catalysts using STM, HRTEM and diffuse reflectance FT infrared and Raman spectroscopy (SERS, RR).
2. Effect of coordinating agents which compete with O_2 for the axial sites of the transition metal in macrocycles.
3. Evaluation of the electrochemical properties of polymer-modified electrodes.

4. O_2 reduction and generation on transition metal oxides including lithiated NiO.

5. Alternative and modified catalyst supports.

6. Exploratory research on new types of electrocatalysts for bifunctional O_2 electrodes.

REFERENCES

1. J. Zagal, R. K. Sen and E. Yeager, J. Electroanal. Chem., 83 (1977) 207.

2. J. Zagal, P. Bindra and E. Yeager, J. Electrochem. Soc., 127 (1980) 1506.

3. S. Zecevic, B. Simic-Glavaski, E. B. Yeager, A.B.P. Lever and P. C. Minor, J. Electroanal. Chem., 196 (1985) 339.

4. A. Elzing, A. Vanderputten, W. Visscher and E. Barendrecht, J. Electroanal. Chem., 233 (1987) 99.

5. B. Z. Nikolic, R. R. Adzic and E. B. Yeager, J. Electroanal. Chem., 103 (1979) 281.

6. B. Simic-Glavaski S. Zecevic and E. B. Yeager, J. Raman Spectrosc., 14 (1983) 338.

7. R. Adzic, B. Simic-Glavaski and E. B. Yeager, J. Electroanal. Chem., 194 (1985) 155.

8. W. A. Nevin, W. Liu, M. Melnik and A.B.P. Lever, J. Electroanal. Chem., 213 (1986) 217.

9. A.B.P. Lever, S. Licoccia and B. S. Ramaswamy, Inorganica Chemica Acta, 64 (1982) L87.

10. S. Gupta and E. Yeager, J. Electroanal. Chem., accepted for publication.

11. A. A. Tanaka, C. Fierro, D. Scherson and E. B. Yeager, J. Phys. Chem., 91 (1987) 3799.

12. J. Randin and E. Yeager, J. Electrochem. Soc., 118 (1971) 711.

13. P. H. Lippel, R. J. Wilson, M. D. Miller, C. Woll and S. Chiang, Phys. Rev. Lett., 62 (1989) 171.

14. B. A. Achar, G. M. Fohler and J. A. Parker, J. Polymer Sci., 20 (1982) 1785.

15. E. Ojadi, R. Selzer and H. Linschitz, J. Am. Chem. Soc., 107 (1985) 7783.

16. D. Chu, Ph.D. Dissertation, Case Western Reserve University, 1989, p. 28.

17. A. Bard and L. R. Faulkner, in Electrochemical Methods, Fundamentals and Applications, Chap. 8, p. 291, John Wiley and Sons, Inc. (1980).

18. D. A. Gough and J. K. Leypoldt, Anal. Chem., 51 (1979) 439.

19. C. P. Andrieur and J. M. Saveant, J. Electroanal. Chem., 134 (1982) 163.

20. D. R. Lawson, L. D. Whiteley and C. R. Martin, J. Electrochem. Soc., 135 (1988) 2247.

21. L. Marcos and E. Yeager, Electrochim. Acta, 15 (1970) 953.

22. H. Jahnke, M. Schonborn and G. Zimmermann, Topics in Current Chemistry,, 135 (1976) 61.

23. Y. Kurimura, E. Tsuchida and M. Kaneko, J. Polym. Sci., 9 (1971) 3511.

LAWRENCE BERKELEY LABORATORY
UNIVERSITY OF CALIFORNIA
INFORMATION RESOURCES DEPARTMENT
BERKELEY, CALIFORNIA 94720